

From Matrix Models and quantum fields to Hurwitz space and the absolute Galois group

Robert de Mello Koch ^{a,1} and Sanjaye Ramgoolam ^{b,2}

^a *National Institute for Theoretical Physics ,
Department of Physics and Centre for Theoretical Physics
University of Witwatersrand, Wits, 2050,
South Africa*

^b *Centre for Research in String Theory, Department of Physics,
Queen Mary University of London,
Mile End Road, London E1 4NS, UK*

ABSTRACT

We show that correlators of the hermitian one-Matrix model with a general potential can be mapped to the counting of certain triples of permutations and hence to counting of holomorphic maps from world-sheet to sphere target with three branch points on the target. This allows the use of old matrix model results to derive new explicit formulae for a class of Hurwitz numbers. Holomorphic maps with three branch points are related, by Belyi's theorem, to curves and maps defined over algebraic numbers $\bar{\mathbb{Q}}$. This shows that the string theory dual of the one-matrix model at generic couplings has worldsheets defined over the algebraic numbers and a target space $\mathbb{P}^1(\bar{\mathbb{Q}})$. The absolute Galois group $Gal(\bar{\mathbb{Q}}/\mathbb{Q})$ acts on the Feynman diagrams of the 1-matrix model, which are related to Grothendieck's Dessins d'Enfants. Correlators of multi-matrix models are mapped to the counting of triples of permutations subject to equivalences defined by subgroups of the permutation groups. This is related to colorings of the edges of the Grothendieck Dessins. The colored-edge Dessins are useful as a tool for describing some known invariants of the $Gal(\bar{\mathbb{Q}}/\mathbb{Q})$ action on Grothendieck Dessins and for defining new invariants.

¹ robert@neo.phys.wits.ac.za

² s.ramgoolam@qmul.ac.uk

Contents

1	Introduction	2
2	One Matrix Model and Hurwitz space	4
2.1	Review : Riemann's existence theorem and Riemann-Hurwitz formula	4
2.2	Brief review of diagrams and tensor space techniques	6
2.3	Gaussian Matrix Model and maps to \mathbb{P}^1 with three branch points	8
2.4	Comments on integrality	10
2.5	Perturbed model, 3 Branch points, and new results on Hurwitz numbers	10
2.6	Universal expressions, Branes and Resolvents	17
3	Feynman Graphs and the absolute Galois group	20
3.1	3 Branch points : The Observable, The Wick contraction and the Product	21
3.2	Belyi's theorem : From Three branch points to $\bar{\mathbb{Q}}$	21
3.3	$Gal(\bar{\mathbb{Q}}/\mathbb{Q})$ for organizing Feynman graphs	23
3.4	Examples	24
3.5	Belyi pairs and square Strebel differentials	29
3.6	Topological string theory on \mathbb{P}^1	30
4	Multi-Matrix models and colored-edge Dessins	31
4.1	Multi-Matrix models	31
4.2	Colored Dessins, permutation triples and subgroups of S_{2n}	32
4.3	Coloring edges to coloring vertices	34
4.4	Sheaves of colored Dessins over Hurwitz space	34
4.5	Hurwitz space and String theory for multi-matrix models	35
5	Colored-edge Dessins as a tool for Galois invariants	35
5.1	From Dessin to list of colored-Dessins and list of multi-matrix operators	35
5.2	Some new combinatoric Galois invariants	38
5.3	Known invariants and edge-colorings of Ribbon graphs	39
6	Summary and Outlook	42
A	Glossary and key facts	46

1 Introduction

Hermitian matrix models (subsequently labeled old matrix models) were the centre of intense research in string theory in the early nineties [1, 2, 3]. This led to connections with 2D topological gravity and intersection theory on $\mathcal{M}_{g,n}$ [4, 5]. A physical picture in terms of string theory in one physical (Liouville) dimension was developed. Some reviews on the subject are [6, 7, 8].

In the mid-nineties, a string theory of two dimensional Yang Mills theory (2dYM) was discovered [9]. Exact answers for partition functions were converted using Schur-Weyl duality, to a $1/N$ expansion where the contribution at each order was expressed in terms of symmetric group data. The simplest way to exhibit the string theory was in the form of Hurwitz spaces of holomorphic maps and Euler characters of these spaces were identified in the large N expansion [13]. A review and references can be found in [14]. Some recent developments include a new understanding of the coupled expansion of 2dYM in terms of holomorphic maps [10], connections between Hurwitz spaces and gauge-string duality in higher dimensions (AdS_3/CFT_2) [11] and instanton based methods for the large order behavior for certain Hurwitz spaces with simple branch points [12].

In this paper we follow the strategy which proved fruitful in constructing the string theory dual of 2dYM : express the computation of correlation functions in hermitian matrix models in terms of symmetric group data and interpret the result in terms of branched covers using classic mathematical results (Riemann existence theorem). The Riemann surfaces appearing as covering spaces are the string worldsheets. The target space of the maps define the target space of the string theory.

In deriving the connection between matrix model correlators and symmetric group data, we find it useful to use diagrammatic tensor space techniques which have found various applications in 2dYM [15] and more recently in AdS/CFT [16, 17, 18, 19, 20, 21, 22]. These techniques have been used to compute Wilson loops in 2dYM, diagonal bases for correlators in the half-BPS sector of $N = 4$ SYM and more general sectors. We review some relevant aspects of the tensor space techniques in section (2.2).

Our first result is a connection between one-point functions of arbitrary multi-trace operators of the one-matrix model and a counting of equivalence classes of **three permutations**. These equivalence classes are defined in (2.1). The Riemann existence theorem relates the counting of strings of permutations to Hurwitz counting problems of holomorphic maps from one Riemann surface to another, with specified branching data. We review this in (2.1).

The importance of Riemann's existence theorem is that it relates a discrete symmetric group counting problem to holomorphic map counting defined in the continuum. The philosophy of the old matrix models was that the Matrix models generate discretized Riemann surfaces. Different scaling limits from these discretizations approach different string backgrounds. Here we are using the Riemann existence theorem to get at a continuum picture

for any correlator for generic potential. Then we are getting the different string backgrounds from the scaling limits of this continuum problem (which admits a mathematically equivalent discrete permutation interpretation).

The fact that three permutations appear in the counting problem means that we are counting branched covers with 3 branch points on the sphere \mathbb{P}^1 , which can be chosen to be at $0, 1, \infty$. The covering space is a Riemann surface, equipped with a map to the target sphere. The inverse image of each branch point contains one or more points on the covering Riemann surface where the derivative of the map vanishes. These are called ramification points. They are each labeled by a positive integer. The branch point is associated with a set of ramification points and thus with a set of positive integers. A remarkable theorem in mathematics [23], the **Belyi theorem**, implies that, for the case of three branch points, the covering curve and the map are **defined over algebraic numbers**. These are numbers which solve polynomial equations with coefficients in \mathbb{Q} , the rational numbers. They give rise to a field $\bar{\mathbb{Q}}$, which is the algebraic closure of \mathbb{Q} . An important group in number theory, called the absolute Galois group $Gal(\bar{\mathbb{Q}}/\mathbb{Q})$ (which we will often call “the Galois group”), acts on $\bar{\mathbb{Q}}$ while leaving \mathbb{Q} fixed) organizes all the key properties of the algebraic numbers [24]. A fact related to Belyi’s theorem, highlighted by Grothendieck, is that the Galois group acts faithfully on the equivalence classes of triples of permutations. He described Dessins D’enfants which capture these equivalence classes. In our case, the triples are coming from Feynman diagrams of the one-matrix model. And in fact the direct connection between Feynman diagrams and Dessins is not hard to see. It is explained in section (3.3). This means that the Galois group acts on the Feynman diagrams, and sets of *Feynman diagrams can be assembled into Galois orbits*. Since the Feynman diagrams also correspond to Hurwitz classes consisting of a string worldsheet and a holomorphic map to \mathbb{P}^1 , we may say that *the Galois group organizes the string worldsheets* contributing to the sum over maps.

We generalize the connection between permutation triples and correlators to multi-matrix models. The Dessins d’Enfants of Grothendieck are replaced by **colored-edge Dessins**. We define the equivalence classes of the colored-edge Dessins in terms of equivalences generated by some subgroups of the permutation group. The continuum data related to the colored Dessins is shown to be richer than just the holomorphic maps f related to the Dessins. It is replaced by pairs (f, s) where the holomorphic map f is accompanied by additional data consisting of sections of sheaves on the covering Riemann surface, supported at some of the ramification points. These pairs are naturally related to sheaves over Hurwitz space. We describe these results in section (4.4).

An important problem considered at length in the Math literature is that of finding **Galois invariants**, properties of Dessins which are invariant under the Galois action. We provide a new construction of Galois invariants using the colored-edge Dessins of the multi-Matrix models. These invariants can be defined in terms of lists of multi-matrix operators, which can be viewed combinatorially as multiple necklaces-with-colored-beads. We also use the colored-edge Dessins to describe some known invariants from the mathematical literature.

It is interesting that the traditional picture of old Matrix Models is that of discretized worldsheet Riemann surfaces for generic potential giving rise to continuum Riemann surfaces in double scaling limits, while the picture developed using Hurwitz space and Belyi's theorem implies that we are getting another kind of "discretization" for generic potentials, namely replacing curves, maps and target space defined over \mathbb{C} with curves, maps and target space defined over $\bar{\mathbb{Q}}$.

Since this paper overlaps with (superficially) disconnected areas of string theory, matrix models and number theory, we collect some key words and facts in the Appendix A, which should be useful to diverse readers.

2 One Matrix Model and Hurwitz space

2.1 Review : Riemann's existence theorem and Riemann-Hurwitz formula

Using local complex coordinates a holomorphic map satisfies $\bar{\partial}_z f = 0$. The Riemann existence theorem relates to the counting of holomorphic maps $f : \Sigma_h \rightarrow \Sigma_T$ between world-sheet Riemann surface Σ_h of genus h and target space Riemann surface Σ_T . In this paper Σ_T will have genus 0, so it is the sphere or complex projective line \mathbb{P}^1 . Two maps f_1 and f_2 are defined to be equivalent if there is a biholomorphic isomorphism $\phi : \Sigma_h \rightarrow \Sigma_h$ such that the following diagram is commutative

$$\begin{array}{ccc} \Sigma_h & \xrightarrow{\phi} & \Sigma_h \\ f_1 \searrow & & \swarrow f_2 \\ & \mathbb{P}^1 & \end{array} \quad (2.1)$$

In other words, equivalent maps f_1, f_2 obey the equation $f_1 = f_2 \circ \phi$ or $f_2 = f_1 \circ \phi^{-1}$. For a generic point on P , the inverse image consists of d points, where d is the degree of the map. For a finite set of points, called **branch points**, there are fewer inverse images. If we consider a small disc around a branch point, the inverse images will be a number of discs. Restricting the map to one of these discs, it looks like $w = z^r$ for some positive integer r . If $r = 1$ the inverse image is an ordinary point. For $r > 1$ it is a **ramification point**. For $r = 2$, it is a simple ramification point. The vector (r_1, r_2, \dots) called the **ramification profile** determines branching numbers $\sum_i (r_i - 1)$. The sum of these over all branch points is denoted as B . The degree of the map is equal to $d = \sum_i i r_i$. The Riemann-Hurwitz theorem states that

$$(2h - 2) = d(2G - 2) + B \quad (2.2)$$

Equivalent maps have the same set of branch points. Given such a holomorphic map (branched cover) with L branch points, we can get a sequence $\sigma_1, \sigma_2, \dots, \sigma_L$ of permutations in S_d . They are obtained by labeling the inverse images of a generic base point, and

following the inverse images of a closed path starting at the base point. For the sphere target, we have

$$\sigma_1 \sigma_2 \cdots \sigma_L = 1 \tag{2.3}$$

which follows from the fact that a path going round all the branch points is contractible. Two equivalent holomorphic maps are described by permutations $\sigma_1, \sigma_2, \dots, \sigma_L$ and $\sigma'_1, \dots, \sigma'_L$ which are related by

$$\sigma_i = \alpha \sigma'_i \alpha^{-1} \tag{2.4}$$

for some fixed $\alpha \in S_d$. This correspondence between sequences of permutations and Holomorphic maps is the **Riemann existence theorem**. This reduces the counting of maps with fixed branch points to a combinatoric problem in permutation groups. Thus a space defined by maps from a smooth space (complex manifold) can be described by the data of branch point locations and some discrete data of permutation counting. For fixed branch points, the continuum problem is entirely reduced to discrete data. We will next show that, precisely this kind of permutation counting arises in the computation of general 1-point functions in the one-matrix model. In fact we always have $L = 3$.

We recap the key points for the case $L = 3$. Holomorphic maps from Riemann surfaces to sphere with three branch points are determined by three permutations $\sigma_1, \sigma_2, \sigma_3$ such that

$$\sigma_1 \sigma_2 \sigma_3 = 1 \tag{2.5}$$

Permutations $(\sigma'_1, \sigma'_2, \sigma'_3)$ determine the same map iff

$$\begin{aligned} \sigma'_1 &= \alpha \sigma_1 \alpha^{-1} \\ \sigma'_2 &= \alpha \sigma_2 \alpha^{-1} \end{aligned} \tag{2.6}$$

for some $\alpha \in S_d$. Because of (2.5), the condition (2.6) suffices to ensure that $\sigma'_3 = \alpha \sigma_3 \alpha^{-1}$. We will refer to $(\sigma_1, \sigma_2, \sigma_3)$ as **Hurwitz data** for a holomorphic map. Equivalence classes under the conjugation (2.6) will be called **Hurwitz classes**.

The counting of triples obeying (2.5) is conveniently written by defining a delta function over symmetric groups. For $\sigma \in S_d$ we define

$$\begin{aligned} \delta_{S_d}(\sigma) &= 1 \text{ if } \sigma = 1, \text{ the identity permutation} \\ &= 0 \text{ if } \sigma \neq 1 \end{aligned} \tag{2.7}$$

By linearity this extends to a delta-function on the group algebra. So counting triples is given by

$$\sum_{\sigma_1, \sigma_2, \sigma_3 \in S_d} \delta_{S_d}(\sigma_1 \sigma_2 \sigma_3) \tag{2.8}$$

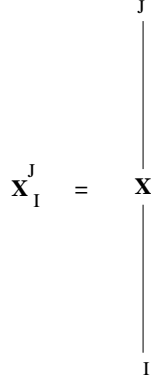


Figure 1: Operator in tensor space and diagram

2.2 Brief review of diagrams and tensor space techniques

It is useful in computations of correlators in matrix theories, to think of the matrices X, Y, Z etc. as operators in a vector space V . Indeed a matrix X is a linear operator on a vector space V . Choosing a basis $|e_i\rangle$ we have

$$X|e_i\rangle = X_i^j|e_j\rangle \quad (2.9)$$

We can extend this to define an action on $V^{\otimes m}$ as follows

$$(X \otimes X \cdots \otimes X)|e_{i_1} \otimes e_{i_2} \otimes \cdots \otimes e_{i_m}\rangle = X_{i_1}^{j_1} \cdots X_{i_m}^{j_m}|e_{j_1} \otimes e_{j_2} \otimes \cdots \otimes e_{j_m}\rangle \quad (2.10)$$

We can write this more compactly, by writing $\mathbf{X} = (X \otimes X \cdots \otimes X)$ and the multi-indices $I = (i_1, i_2, \cdots, i_m)$

$$\mathbf{X}|e_I\rangle = \mathbf{X}_I^J|e_J\rangle \quad (2.11)$$

By introducing dual vectors, we may also write

$$\langle e^J|\mathbf{X}|e_I\rangle = \mathbf{X}_I^J \quad (2.12)$$

Many manipulations are conveniently conducted by using diagrams. The first step is simply to write the above operator in tensor space as in the Figure 1.

The strands represent the states (vectors) of $V^{\otimes m}$.

Different traces and products of traces of X , such as $(tr X)^2 tr(X^2)$ can be written by composing the action of \mathbf{X} with that of permutations $\sigma \in S_m$ acting as

$$\sigma|e_{i_1} \otimes e_{i_2} \otimes \cdots \otimes e_{i_m}\rangle = |e_{i_{\sigma(1)}} \otimes e_{i_{\sigma(2)}} \otimes \cdots \otimes e_{i_{\sigma(m)}}\rangle \quad (2.13)$$

For example

$$tr(X^2) = tr_{V^{\otimes 2}}((X \otimes X)(12)) = tr_{V^{\otimes 2}}((12)(X \otimes X)) \quad (2.14)$$

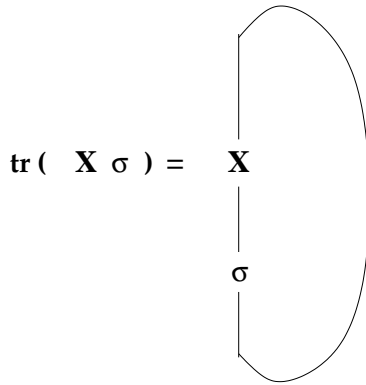


Figure 2: Multitrace operators

while replacing (12) by the identity permutation gives $(\text{tr}X)^2$. In the diagrammatic representation of tensor space manipulations, tracing is drawn by joining strands. Any multi-trace operator with m copies of X can be obtained from an appropriate permutation of the strands. This is shown in Figure 2. Two permutations which are conjugate to each other give rise to the same multi-trace operator. There is a one-one correspondence between multi-traces and conjugacy classes of permutations.

In quantum field theory X is a function of space-time coordinates, and in fact an operator in a Hilbert space, hence the terminology “multi-trace operators”. Matrix models where X depends on no coordinates at all are special cases of QFT in zero space-time dimensions. Most of this paper is indeed focused on that case, but diagrammatic tensor space techniques are useful more generally. The key element of free QFT (Gaussian matrix models) we will use is that observables are correlators of multi-traces and these can be computed by combining Wick’s theorem with the basic formula

$$\langle X_j^i X_l^k \rangle = \delta_l^i \delta_j^k \quad (2.15)$$

Wick’s theorem implies that for a correlator involving a large number of X ’s we need to sum

$$\langle X_{j_1}^{i_1} X_{j_2}^{i_2} \cdots X_{j_{2n}}^{i_{2n}} \rangle = \sum_{\gamma \in [2^n]} \delta_{j_{\gamma(1)}}^{i_1} \delta_{j_{\gamma(2)}}^{i_2} \cdots \delta_{j_{\gamma(2n)}}^{i_{2n}} \quad (2.16)$$

The permutation γ is being summed over all elements in the conjugacy class of S_{2n} with n cycles of length 2. The size of the conjugacy class is $\frac{(2n)!}{2^n n!}$ which is the number of ways of choosing n pairs from $2n$ objects. The equation (2.16) is expressed diagrammatically in Figure 3.

For computations in Gaussian multi-matrix models, involving matrices $X, Y, Z \cdots$, the correlator of a pair of different matrices is zero, and for each pair of like matrices we have the correlator in (2.15). Again, the above remark that multi-traces can be obtained by composing permutations with an appropriate operator in tensor space holds true. Multi-traces with

$$\langle \mathbf{X} \rangle = \sum_{\gamma} \gamma$$

Figure 3: Correlator using Wick's theorem : γ in $[2^n]$ (see text for further explanation)

m_1, m_2, m_3 copies of X, Y, Z are obtained from $\mathbf{X} \otimes \mathbf{Y} \otimes \mathbf{Z}$ acting on $V^{\otimes m_1+m_2+m_3}$. While in the case of the single matrix model, conjugations by permutations in S_m lead to the same operator, here conjugations by permutations in the subgroup $S_{m_1} \times S_{m_2} \times S_{m_3}$ lead to the same multi-matrix operator. For a non-zero correlator, we need m_1, m_2, m_3 to be even, so we write $m_1 = 2n_1, m_2 = 2n_2, m_3 = 2n_3$. Wick's theorem results in sums over permutations γ in $[2^{2n_1}, 2^{2n_2}, 2^{2n_3}]$ of $S_{2n_1} \times S_{2n_2} \times S_{2n_3}$.

Some recent papers where diagrammatic tensor space techniques play an important role include [19, 20, 21, 22, 25, 26, 27].

2.3 Gaussian Matrix Model and maps to \mathbb{P}^1 with three branch points

Choose a permutation $\sigma \in S_{2n}$ which characterizes a multi-trace operator with $2n$ copies of X . The correlator only depends on the conjugacy class $[\sigma]$ of σ . Compute the correlator in the Gaussian matrix model which has the two point function

$$\langle X_j^i X_l^k \rangle = \delta_l^i \delta_j^k \tag{2.17}$$

Using this two point function and Wick's theorem (2.16), we have

$$\begin{aligned} \langle tr_{2n}(\sigma \mathbf{X}) \rangle &= \sum_{\gamma \in [2^n]} tr_{2n}(\gamma \sigma) \\ &= \sum_{\gamma \in [2^n]} N^{C_{\gamma \sigma}} \\ &= \sum_{\tau \in S_{2n}} \sum_{\gamma \in [2^n]} N^{C_{\tau}} \delta_{S_{2n}}(\sigma \gamma \tau) \end{aligned} \tag{2.18}$$

Here $[2^n]$ is the conjugacy class with n cycles of length 2 and $C_{\gamma \sigma}$ is the number of disjoint cycles in the permutation $\gamma \sigma$.

A judicious choice of normalization gives

$$\begin{aligned} & \frac{||[\sigma]||}{(2n)!} N^{C_\sigma - n} \langle tr_{2n}(\sigma X) \rangle \\ &= \frac{1}{(2n)!} \sum_{\tau \in S_{2n}} \sum_{\sigma \in [\sigma]} \sum_{\gamma \in [2^n]} \delta_{S_{2n}}(\sigma\gamma\tau) N^{C_\sigma + C_\tau - n} \end{aligned} \quad (2.19)$$

In the above $||[\sigma]||$ is the size of the conjugacy class $[\sigma]$. $b(\sigma) = 2n - C_\sigma$ is the branching number of the permutation, which only depends on the conjugacy class of the permutation. $b([2^n])$ is the branching number of the conjugacy class with n cycles of length 2, which is equal to n .

The above sum counts branched covers of the sphere, with 3 branched points, described by permutations σ, γ, τ . The power of N keeps track of the genus of the worldsheet

$$\begin{aligned} (2 - 2h) &= 2n(2 - 2G) - B \\ &= 4n - (2n - C_\sigma) - (2n - C_\tau) - (2n - C_{[2^n]}) \\ &= C_\sigma + C_\tau - n \end{aligned} \quad (2.20)$$

where G is the genus of the target, in this case 0, and B is the total branching number. Using (2.20) and (2.19) we have

$$\frac{||[\sigma]||}{(2n)!} N^{C_\sigma - n} \langle tr_{2n}(\sigma X) \rangle = \sum_{f([\sigma], [2^n]): \Sigma_h \rightarrow \mathbb{P}^1} \frac{1}{|Aut f|} N^{2-2h} \quad (2.21)$$

The sum is over the branched covers with three branch points. The first branch point is described by permutations σ in the conjugacy class $[\sigma]$ defined by the observable $tr_{2n}(\sigma \mathbf{X})$. The second branch point, resulting from Wick contractions, is described by permutations γ in the conjugacy $[2^n]$. The third branch point can be in any conjugacy class which arises in the product of σ and γ . Given two maps

$$\begin{aligned} \phi &: \Sigma_h \rightarrow \Sigma_h \\ f &: \Sigma_h \rightarrow \mathbb{P}^1 \end{aligned} \quad (2.22)$$

we say that $\phi \in Aut(f)$ if

$$f \circ \phi = f \quad (2.23)$$

To obtain the result (2.21) we have used the fact that the sum over σ, γ and τ of $\delta_{S_{2n}}(\sigma\gamma\tau)$ with a factor of $\frac{1}{(2n)!}$, is equal to the sum over maps $f(\sigma, \mathbf{T}) : \Sigma_h \rightarrow \mathbb{P}^1$ with each map weighted by $\frac{1}{|Aut f|}$ [9, 14].

If we sum over $[\sigma]$ with the above weights we can define a generating function

$$\mathcal{F}(N) = \sum_n \sum_{[\sigma] \in [S_{2n}]} \frac{||[\sigma]||}{(2n)!} N^{C_\sigma - n} \langle tr_{2n}(\sigma X) \rangle$$

$$= \sum_{f([2^n]): \Sigma_h \rightarrow P_1} \frac{1}{|Aut f|} N^{2-2h} \quad (2.24)$$

Here the sum is over maps, with three branch points, one with ramification profile $[2^n]$, and the other two arbitrary, and weighted correctly (as in string theory) by the worldsheet genus.

2.4 Comments on integrality

Considering (2.21) and (2.18) and noting that $\frac{(2n)!}{|\sigma|}$ is the number of permutations α in S_{2n} which leave σ fixed under conjugations, i.e $\alpha\sigma\alpha^{-1} = \sigma$, we can write this factor as $|Aut(\sigma)|$. This indicates that it is the order of the subgroup $Aut(\sigma)$ of S_{2n} which leave σ fixed under conjugation. Hence we can write

$$\langle tr_{2n}(\sigma X) \rangle = \sum_{\sigma \in [\sigma]} \sum_{\gamma \in [2^n]} N^{C_{\gamma\sigma}} \frac{|Aut(\sigma)|}{|Aut f_{\sigma,\gamma}|} \quad (2.25)$$

$f_{\sigma,\gamma}$ is a Hurwitz class determined by the pair σ, γ . We know that the LHS is an integer times a power of N because it is a sum over Wick contractions. We can also see this directly from the RHS because $Aut f_{\sigma,\gamma} = Aut(\sigma) \cap Aut(\gamma)$ which means that it is a subgroup of $Aut(\sigma)$, hence by group theory must have an order which divides $|Aut(\sigma)|$. For the same reason, using $|Aut(\gamma)| = 2^n n!$, we have $\frac{2^n n!}{|Aut f_{\sigma,\gamma}|}$ is an integer, which means

$$\frac{2^n n!}{|Aut(\sigma)|} \langle tr_{2n}(\sigma X) \rangle \quad (2.26)$$

is a sum of positive integers.

The factor $\frac{|Aut(\sigma)|}{|Aut f_{\sigma,\gamma}|}$ appearing in (2.25) has a nice interpretation. Fix a σ to describe our operator. Pick a γ which determines a Wick contraction. The pair (σ, γ) determines a Hurwitz class. As γ runs over its conjugacy class, we sum over Wick contractions. How many of these Wick contractions are in the same equivalence class as (σ, γ) ? We can get other permutations $\tilde{\gamma}$ in the conjugacy class of γ by conjugating with $h \in S_{2n}$. Note that other representatives of the same Hurwitz class are related to σ, γ as $(h\sigma h^{-1}, h\gamma h^{-1})$. As we are summing over γ with σ fixed, we are running over pairs $(\sigma, h\gamma h^{-1})$. For this to be equivalent to $(\sigma, \tilde{\gamma})$ we need h to fix σ , i.e $h \in Aut(\sigma)$. But if $h \in Aut(\gamma)$ as well, then it does not change the pair. So the number of Wick contractions which give contributions from the same Hurwitz class as the one of σ, γ is $Aut(\sigma)/Aut f_{\sigma,\gamma}$. Finally, the group that leaves σ and γ fixed is clearly a subgroup of $Aut(\sigma\gamma)$ so that $\frac{|Aut(\sigma\gamma)|}{|Aut f_{\sigma,\gamma}|}$ is also an integer.

2.5 Perturbed model, 3 Branch points, and new results on Hurwitz numbers

In this section we will perturb the Gaussian matrix model, with a potential of the form $\text{Tr}(X^n)$. Expanding the exponential of the perturbation, we see that the partition function

of the perturbed model can be computed by summing over correlators in the Gaussian model, with insertions of powers of $\text{Tr}(X^n)$. At each order in the coupling constant, we have the correlator of a multi-trace operator in the Gaussian model, which as shown in section (2.3), amounts to summing over Hurwitz classes with three branch points. These Hurwitz classes have a permutation σ in the conjugacy class $[n^m]$ coming from the operator insertion, a permutation γ in the conjugacy class $[2^{\frac{nm}{2}}]$ from the Wick contraction and a permutation τ which is the product $\gamma^{-1}\sigma^{-1}$.

2.5.1 Perturbation by $\text{tr}X^4$ and Hurwitz numbers

For concreteness we start with perturbation by $\text{tr}X^4$

$$Z(X) = \int dX e^{-N(\frac{1}{2}\text{tr}X^2 + \frac{g^2}{4}\text{tr}X^4)} \quad (2.27)$$

The free two-point function is

$$\begin{aligned} & \langle X_j^i X_l^k \rangle_0 \\ &= \int dX e^{-\frac{N}{2}\text{tr}X^2} X_j^i X_l^k \\ &= \frac{1}{N} \delta_l^i \delta_j^k \\ &= \frac{1}{N} \langle X_j^i X_l^k \rangle \end{aligned} \quad (2.28)$$

This is the same as (2.17) up to an immaterial factor of $\frac{1}{N}$.

Expanding the exponential

$$\begin{aligned} Z(X) &= \sum_k \int dX e^{-\frac{N}{2}\text{tr}X^2} \frac{(-Ng^2\text{tr}X^4)^k}{4^k k!} \\ &= \sum_k \frac{(-g^2)^k N^k}{4^k k!} \langle (\text{tr}(X^4))^k \rangle_0 \\ &= \sum_k \frac{(-g^2)^k N^k}{4^k k!} \langle \text{tr}_{4k}(\sigma \mathbf{X}) \rangle_0 \end{aligned} \quad (2.29)$$

We have used the observation from section 2.2 that multi-traces can be written as a trace in a tensor product space with a permutation inserted. In this case, $(\text{tr}(X^4))^k$ can be written as a trace in $V^{\otimes 4k}$, which is indicated by the subscript in tr_{4k} . The permutation σ has k cycles of length 4. So $C_\sigma = k$. We can now write

$$\begin{aligned} Z(X) &= \sum_k \frac{(-g^2)^k}{(4k)!} N^{C_\sigma} \frac{(4k)!}{4^k k!} \langle \text{tr}_{4k}(\sigma \mathbf{X}) \rangle_0 \\ &= \sum_k \frac{(-g^2)^k}{(4k)!} N^{C_\sigma} \sum_{\sigma \in [4^k]} \langle \text{tr}_{4k}(\sigma \mathbf{X}) \rangle_0 \end{aligned}$$

$$\begin{aligned}
&= \sum_k \frac{(-g^2)^k}{(4k)!} N^{C_\sigma - 2k} \sum_{\sigma \in [4^k]} \sum_{\gamma \in [2^k]} \sum_{\tau \in S_{4k}} \text{tr}_{4k}(\sigma\gamma) \\
&= \sum_k \frac{(-g^2)^k}{(4k)!} \sum_{\sigma \in [4^k]} \sum_{\gamma \in [2^k]} \sum_{\tau \in S_{4k}} \delta_{S_{4k}}(\sigma\gamma\tau) N^{C_\sigma + C_\tau - 2k} \\
&= \sum_k (-g^2)^k \sum_{f([4^k], [2^{2k}]): \Sigma_h \rightarrow \mathbb{P}^1} \frac{1}{|\text{Aut}(f([4^k], [2^{2k}]))|} N^{2-2h} \tag{2.30}
\end{aligned}$$

The factor $|\sigma|$ we needed in (2.19) arose naturally as a result of expanding the standard normalization of the potential in the Matrix Model.

For any g we have a Hurwitz interpretation of the Matrix model correlator. As g approaches g_c the partition functions diverges and the standard string interpretation of the 90's emerges i.e CFT coupled to pure $c \leq 1$ matter. In this case, it is just pure gravity. Very importantly now we also have an interpretation in terms of **continuum worldsheets and holomorphic maps for any g** .

The double-scaled string theory (see the review [8]) related to the pure gravity arises in the limit,

$$g \rightarrow g_c = -\frac{1}{12} \tag{2.31}$$

where it can be proved that

$$Z_h \sim (g_c - g)^{\frac{5\chi_h}{2}} \tag{2.32}$$

and where it becomes appropriate to define a new genus counting parameter

$$\kappa^{-1} = N(g - g_c)^{5/4} \tag{2.33}$$

Our results imply that *2D gravity coupled to different minimal models arises from critical limits of generating functions of Hurwitz numbers*.

Fluctuations in the matrix model are of size $\frac{1}{N^2}$. By switching to eigenvalue variables, one can use a classical (saddle point) analysis to extract the leading large N behavior. This will give Hurwitz numbers for maps with both worldsheet and target a sphere. Let us make this explicit. The large N eigenvalue density for this model has been calculated [28]

$$\rho(\lambda) = \frac{1}{2\pi g} (\lambda^2 + 1 + \frac{1}{2}a^2) \sqrt{(a^2 - \lambda^2)} \tag{2.34}$$

where

$$a^2 = \frac{2}{3}(-1 + \sqrt{1 + 12g}).$$

The free energy is given as usual by the log of the partition function Z . For the model we consider here

$$F = N^2 \left(\int d\lambda d\mu \rho(\lambda) \rho(\mu) \log |\lambda - \mu| - \frac{1}{g} \int d\lambda \rho(\lambda) \left(\frac{\lambda^2}{2} + \frac{\lambda^4}{4} \right) \right) \tag{2.35}$$

Using the explicit eigenvalue density the free energy is evaluated to obtain [28]

$$\frac{F(g) - F(0)}{N^2} = \sum_{k=1}^{\infty} g^k \frac{(-1)^{k+1} (2k-1)! 6^k}{2k(k+2)!}.$$

This free energy can be recovered by summing the connected planar diagrams. To make sure we pick the connected part in the delta function $\delta(\sigma\gamma\tau)$ appearing in (2.30), we keep only triples σ, γ, τ which are transitive. To be more precise, the coefficient of g^k in the free energy is the number of times $\sigma\gamma = \tau^{-1}$ for (i) σ summed over $[4^k]$ (ii) γ summed over $[2^{2k}]$ and (iii) the group generated by σ, γ, τ acts transitively on the set $\{1, 2, \dots, 4k\}$. In other words σ, γ, τ generate the whole of S_{4k} . In what follows we use the notation $H_{\alpha, \beta}^g$ to denote the number of degree d branched covers of \mathbb{P}^1 by a genus g connected Riemann surface with three branch points, the first two having ramification profiles α and β , and the third having arbitrary ramification. If the cover has automorphism group $\text{Aut} f_{\sigma, \gamma}$ it is counted with multiplicity $1/|\text{Aut} f_{\sigma, \gamma}|$. This notation coincides with that of [29]. The Hurwitz number $H_{[2^{2k}], [4^k]}^0$ is given by the absolute value of the coefficient of g^k in the free energy. From the free energy above

$$\boxed{H_{[2^{2k}], [4^k]}^0 = \frac{(2k-1)! 6^k}{2k(k+2)!}} \quad (2.36)$$

In terms of delta functions

$$\sum_{\sigma \in [4^k]} \sum_{\gamma \in [2^{2k}]} \sum_{\tau \in S_{4k}: C_{\tau} = k+2} \frac{1}{(4k)!} \delta^{(conn:0)}(\sigma\gamma\tau) = \frac{(2k-1)! 6^k}{2k(k+2)!} \quad (2.37)$$

The superscript *conn* on the delta functions indicating that we are restricting to transitive triples which give rise to connected covers. The superscript 0 indicates that we are restricting to genus zero worldsheet, which is equivalent (see (2.20)) to restricting $C_{\tau} = 2k + 2$.

By expanding the partition function itself, we can obtain the Hurwitz numbers $\tilde{H}_{[2^{2k}], [4^k]}^0$ which are defined as before except that the covers need not be connected. Finally, correlators at large N are given as moments of the large N eigenvalue density. For an arbitrary $2j$ cycle¹ σ we have

$$\frac{1}{N^j} \int dX \text{tr}_{2j}(\sigma \mathbf{X}) e^{-N(\frac{1}{2} \text{tr} X^2 + \frac{g^2}{4N} \text{tr} X^4)} = \int_{-a}^a d\lambda \rho(\lambda) \lambda^{2j}$$

Expanding this correlator in powers of g^k , the expansion coefficients are related to $\tilde{H}_{[2^{2k+2j}], [\sigma \circ 4^k]}^0$.

2.5.2 Perturbation by $\text{tr}(X^3)$ and Hurwitz numbers

To obtain the Hurwitz numbers $H_{[2^{3k}], [3^{2k}]}^0$ we consider the matrix model

$$Z(X) = \int dX e^{-N(\frac{1}{2} \text{tr} X^2 + \frac{g}{3} \text{tr} X^3)}. \quad (2.38)$$

¹We assume that σ has a single cycle. Using the large N eigenvalue density one is only able to compute the leading contribution to any given correlator. This is disconnected if σ is not a single cycle.

For this model [28],

$$\frac{F(g) - F(0)}{N^2} = -\frac{1}{2} \sum_{k=1}^{\infty} \frac{(8g^2)^k}{(k+2)!} \frac{\Gamma(3k/2)}{\Gamma(k/2+1)},$$

so that

$$\boxed{H_{[2^{3k}], [3^{2k}]}^0 = \frac{1}{2} \frac{8^k}{(k+2)!} \frac{\Gamma(3k/2)}{\Gamma(k/2+1)}}. \quad (2.39)$$

In terms of delta functions

$$\sum_{\sigma \in [3^{2k}]} \sum_{\gamma \in [2^{3k}]} \sum_{\tau \in S_{6k}: C_\tau = k+2} \frac{1}{(6k)!} \delta^{(\text{conn}:0)}(\sigma\gamma\tau) = \frac{1}{2} \frac{8^k}{(k+2)!} \frac{\Gamma(3k/2)}{\Gamma(k/2+1)} \quad (2.40)$$

The connectedness condition is a transitivity constraint on the triples, the genus zero condition is equivalent to $C_\tau = 2 + k$.

2.5.3 Perturbation by $\text{tr}X^6$ and Hurwitz numbers

Finally, we consider the matrix model with $\text{tr}X^6$ potential

$$Z(X) = \int dX e^{-N(\frac{1}{2}\text{tr}X^2 + \frac{g}{6}\text{tr}X^6)}. \quad (2.41)$$

The large N limit for this model has been studied in [30]. From [30] we obtain the free energy

$$F = \frac{-a^4}{12} + \frac{7}{12}a^2 - \frac{1}{2} \log a^2$$

where

$$\hat{g}a^6 + a^2 - 1 = 0 \quad \hat{g} = 60g$$

Using these two equations we will now develop the series expansion of the free energy. This last cubic is easily solved to give

$$a^2 = \frac{1}{\sqrt{3\hat{g}}} \left(\sqrt{1 + \frac{27\hat{g}}{4}} + \sqrt{\frac{27\hat{g}}{4}} \right)^{\frac{1}{3}} - \frac{1}{\sqrt{3\hat{g}}} \left(\sqrt{1 + \frac{27\hat{g}}{4}} - \sqrt{\frac{27\hat{g}}{4}} \right)^{\frac{1}{3}} \quad (2.42)$$

We know that we have the correct root because it is clear that a^2 has an expansion starting at 1 for small \hat{g} . It is now easy to obtain the following series expansions

$$a^2 = \sum_{k=0}^{\infty} \binom{3k}{k} \frac{1}{2k+1} (-1)^k \hat{g}^k \quad (2.43)$$

$$a^4 = \sum_{k=0}^{\infty} \frac{(3k+1)!}{(2k+1)!(k+1)!} (-1)^k \hat{g}^k$$

and

$$\log(a^2) = \sum_{k=1}^{\infty} (-1)^k \frac{(3k-1)!}{k!(2k)!} \hat{g}^k$$

Collecting these results we obtain

$$\frac{F(g) - F(0)}{N^2} = \sum_{k=1}^{\infty} \frac{(-1)^{k+1}}{2} \frac{(10)^k (3k-1)!}{(2k+1)!(k+1)!} g^k \quad (2.44)$$

and hence the Hurwitz numbers

$$\boxed{H_{[2^{3k}], [6^k]}^0 = \frac{1}{2} \frac{(10)^k (3k-1)!}{(2k+1)!(k+1)!}} \quad (2.45)$$

To check our result (2.44), we will now explain how the free energy, or equivalently, Hurwitz numbers, can be computed from the class algebra coefficients of the symmetric group. Return to the formula (2.18)

$$\begin{aligned} \langle \text{tr}_{2n}(\sigma X) \rangle &= \frac{1}{|[\sigma]|} \sum_{\rho \in [\sigma]} \sum_{\gamma \in [2^n]} \sum_{\tau \in S_{2n}} N^{C_\tau} \delta_{S_{2n}}(\rho \gamma \tau) \\ &= \sum_{[\tau]} f_{\sigma, \gamma}^\tau \frac{\text{Sym}([\sigma])}{\text{Sym}([\tau])} \end{aligned} \quad (2.46)$$

where $f_{\sigma, \gamma}^\tau$ are the class algebra coefficients

$$T_\sigma T_\gamma = f_{\sigma, \gamma}^\tau T_\tau$$

In this last expression, T_ψ stands for the sum of elements in the conjugacy class $[\psi]$. The class algebra coefficients are easily evaluated with the help, for example, of the Symmetrica program [31].

The partition function is

$$Z = 1 - \frac{gN}{6} \langle \text{tr}(X^6) \rangle_0 + \frac{1}{2!} \left(\frac{gN}{6} \right)^2 \langle \text{tr}(X^6)^2 \rangle_0 + \dots$$

To evaluate $\langle \text{tr}(X^6) \rangle_0$ we need to consider the product

$$[\sigma][\gamma] = [6][2^3] = 6[3^1 3^1] + 8[2^2 1^2] + 5[5^1 1] + 4[4^1 2] + 3[3^2] \quad (2.47)$$

The first two terms on the right hand side each correspond to cycles with 4 parts ($C_\tau = 4$) so these give the leading (planar) contribution. The remaining four terms give a torus (down by $\frac{1}{N^2}$) correction. It is in fact straightforward to identify each of the terms above with a particular double line diagram. Our original operator $\text{tr}(X^6)$ is a sum over 6 indices. We will represent each index by a dot, as shown in Figure 4. These are the object that are permuted by S_6 .

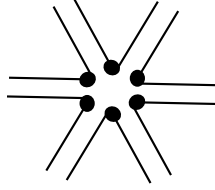


Figure 4: The graphical representation of $\text{tr}(X^6)$.

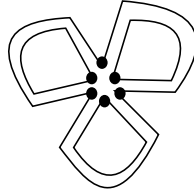


Figure 5: For this double-line diagram $\tau = [1^3 3]$.

To obtain the double line diagram, the 6 “stubs” must be connected by fat (double line) propagators. One such connection is shown in 5 below. The connected double line diagram is in fact a graphical representation of τ . To read τ from this double line diagram, recall that each dot is an object that gets permuted. Each closed loop in the double line diagram will contain at least one dot. These loops tells you how the dots are permuted by the action of S_6 . Thus a loop with n -dots in it corresponds to a n -cycle in τ . For the double line diagram in Figure 5 it is clear that $\tau = [1^3 3]$. From (2.47) we see that the relevant group algebra coefficient is 6 and hence this diagram has a coefficient

$$f_{[6][2^3]}^{[1^3 3]} \frac{\text{Sym}([\sigma])}{\text{Sym}([\tau])} = 6 \frac{6}{3 \cdot 3!} = 2$$

For the double line diagram in Figure 6 it is clear that $\tau = [1^2 2^2]$ and hence this diagram has a coefficient

$$f_{[6][2^3]}^{[1^2 2^2]} \frac{\text{Sym}([\sigma])}{\text{Sym}([\tau])} = 8 \frac{6}{2^2 2! \cdot 1^2 2!} = 3$$

The non-planar double line diagrams are shown in Figure 7. They correspond to $\tau = [3 3]$, $\tau = [4 2]$ and $\tau = [1 5]$ respectively. Notice that each term in (2.47) corresponds to a unique double line diagram. At higher orders in g this is no longer the case - there may be two different double line diagrams with the same cycle structure for τ .

It is now simple to obtain

$$Z = 1 - \frac{g}{6}(5N^4 + 10N^2) + \frac{g^2}{36 \cdot 2!}(700N^6 + O(N^4)) + O(g^3)$$

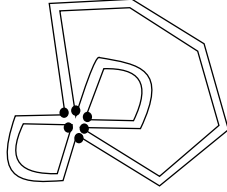


Figure 6: For this double-line diagram $\tau = [1^2 2^2]$.

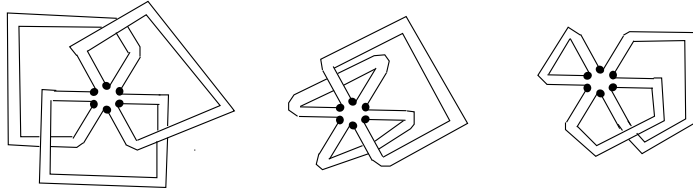


Figure 7: Non-planar double-line diagrams contributing to $\langle \text{tr}(X^6) \rangle$

The free energy is obtained by summing connected diagrams. To get the connected diagrams, take the log

$$\begin{aligned} \log(Z) &= -\frac{g}{6}(5N^4+10N^2)+\frac{g^2}{36 \cdot 2!}(700N^6+\dots)+\dots -\frac{1}{2}\left(-\frac{g}{6}(5N^4+10N^2)+\frac{g^2}{36 \cdot 2!}(700N^6+\dots)+\dots\right)^2+\dots \\ &= -5\frac{gN^4}{6} + 25\frac{g^2N^6}{3} + \dots \end{aligned}$$

This matches the free energy computation above.

We can state the result in terms of the delta functions on symmetric groups

$$\sum_{\rho \in [6^k] \in S_{6k}} \sum_{\gamma \in [2^{3k}] \in S_{6k}} \sum_{\tau \in S_{6k}: C_\tau = 2+2k} \frac{1}{(6k)!} \delta^{(conn; h=0)}(\rho \gamma \tau) = \frac{1}{2} \frac{(10)^k (3k-1)!}{(2k+1)!(k+1)!} \quad (2.48)$$

The superscripts on the delta function indicate that we are restricting to genus zero connected maps. The constraint of the worldsheet being connected is implemented by requiring that the σ, γ, τ generate the whole symmetric group S_{6k} .

2.6 Universal expressions, Branes and Resolvents

Having shown (section (2.3)) that the 1-point function of any multi-trace operator in the Gaussian model counts holomorphic maps with three branch points, it is clear that the partition function and correlation functions of the Gaussian model perturbed by a general potential can likewise be expressed in terms of holomorphic map counting with three branch points. It suffices to just treat the exponential of the perturbation as an observable in the

Gaussian model. Indeed we have seen explicit examples in section (2.5). It is possible to express this simple consideration in elegant formulae if we introduce some definitions.

Given two permutation groups S_{n_1} and S_{n_2} , we can define a canonical embedding of $S_{n_1} \times S_{n_2}$ into $S_{n_1+n_2}$, by considering S_{n_1} as permutations of $\{1 \cdots n_1\}$ and S_{n_2} as permutations of $\{n_1 + 1, \cdots, n_1 + n_2\}$. Given two permutations σ_1, σ_2 respectively in S_{n_1} and S_{n_2} we write $\sigma_1 \circ \sigma_2$. We will call this the outer product of the two permutations. This operation can clearly be extended to an arbitrary string of permutation groups.

We can define an *outer-exponential* of a permutation $\sigma \in S_i$ as follows

$$\mathbf{e}_\circ^\sigma = \sum_{k=0}^{\infty} \frac{1}{k!} \sigma^{\circ k} \quad (2.49)$$

where $\sigma^{\circ k} \equiv \sigma \circ \sigma \circ \cdots \circ \sigma$ is using the embedding of $S_i^{\times k}$ in S_{ki} . The definition can be extended, by linearity and distributivity of the outer product over sums, to the outer exponential of a sum of permutations.

$$\mathbf{e}_\circ^{\sum_i g_i \sigma_i} = \sum_{k=0}^{\infty} \sum_{i_1, i_2, \dots, i_k} \frac{g_{i_1} g_{i_2} \cdots g_{i_k}}{k!} \sigma_{i_1} \circ \sigma_{i_2} \circ \cdots \circ \sigma_{i_k} \quad (2.50)$$

Another useful definition will be a generalization of the delta functions for multiple permutations in the same symmetric group (2.7) to a delta function, denoted $\boldsymbol{\delta}$, which takes three arguments in symmetric groups $S_{d_1}, S_{d_2}, S_{d_3}$ of permutations of $\{1, 2, \cdots, d_1\}, \{1, 2, \cdots, d_2\}$ and $\{1, 2, \cdots, d_3\}$ where the d_i are arbitrary positive integers. If the degrees are not equal the delta function is defined to be zero. When the degrees are equal the $\boldsymbol{\delta}$ is defined as equal to the usual δ_{S_d} . In other words it is equal to 1 if the three permutations are in the same S_d and multiply to 1.

Calculations similar to those involved in (2.19) and (2.30) lead in the case of a perturbation of the Gaussian term by $g \text{Tr} X^i$ as

$$Z = \boldsymbol{\delta} (\mathbf{e}_\circ^{g c_i} \mathbf{T} \boldsymbol{\Omega}) \quad (2.51)$$

Here c_i is a cyclic permutation of length i in S_i . \mathbf{T} is a sum of permutations in $[2^p]$ which is itself summed over p . As p increases S_{2p} viewed as permutations of $\{1, 2, \cdots, 2p\}$, which can be viewed as a subgroup of S_∞ .

$$\mathbf{T} = \sum_p \sum_{\gamma \in [2^p] \in S_{2p}} \gamma \quad (2.52)$$

Similarly

$$\boldsymbol{\Omega} = \sum_p \sum_{\tau \in S_p} N^{C_\tau} \tau \quad (2.53)$$

Keeping track of all the factors of N from normalizations of the perturbations and 2-point function as done in the previous examples shows that the power of N is consistent with a string interpretation according to the Riemann-Hurwitz formula. Likewise, the combinatoric factors lead to $\frac{1}{|\text{Autf}|}$.

A general potential $\text{tr}(X^2) + V(X)$ is naturally associated with a sequence of formal sums of permutations. Usually one considers single trace terms in the potential, so that the $\hat{V} = \sum_i g_i c_i$ is a sum over single cycles. For multi-trace perturbations we have a sum of more general permutations and $\hat{V} = \sum_i g_i \sigma_i$. In this case the partition function is

$$Z = \langle 1 \rangle_{\text{tr}X^2+V} = \boldsymbol{\delta}(\mathbf{e}_\circ^{\hat{V}} \mathbf{T} \mathbf{\Omega}) \quad (2.54)$$

The expansion of the exponential according to (2.50) contains terms in permutation groups of different degrees. For all the terms of a fixed degree d , the definition of $\boldsymbol{\delta}$ picks out from the sums in \mathbf{T} and $\mathbf{\Omega}$ precisely those terms which belong to symmetric groups of the same degree d . Then $\boldsymbol{\delta}$ reduces to a sum over d of terms δ_{S_d} .

This extended language of $\boldsymbol{\delta}, \mathbf{T}, \mathbf{\Omega}$ allows us to give neat expressions for some key quantities in Matrix theory. Consider the function $\text{Det}(x - X)$. Using the earlier manipulations we can write

$$\langle \text{Det}(x - X) \rangle_{\text{tr}X^2+V} = \boldsymbol{\delta}(D \circ \mathbf{e}_\circ^{\hat{V}} \mathbf{T} \mathbf{\Omega}) \quad (2.55)$$

where $D = \sum_i x^{N-i} (-1)^i \sum_{\sigma \in S_i} (-1)^\sigma$. This uses the expansion of the determinant

$$\langle \text{Det}(x - X) \rangle = \sum_i x^{N-i} (-1)^i \langle \chi_{[1^i]}(X) \rangle \quad (2.56)$$

where $\chi_{[1^i]}(X)$ is the Schur polynomial for the representation of $U(N)$ corresponding to the anti-symmetric Young diagram which is a column of length i or equivalently i rows of length 1 as indicated by $[1^i]$. The Schur polynomial has an expansion

$$\chi_{[1^i]}(X) = \sum_{\sigma \in S_i} \frac{(-1)^\sigma}{i!} \text{Tr}_i(\sigma \mathbf{X}) \quad (2.57)$$

where $(-1)^\sigma$ is 1 if the permutation is even and -1 if it is odd.

The 1-point function $\langle \text{Det}(x - X) \rangle$ defines the Baker-Akhiezer function which is used in [32] to argue that the target space of the 1-Matrix model is \mathbb{P}^1 . This conclusion is reached by identifying the insertion of the exponentiated macroscopic loop operator $\exp(\text{Tr} \log(x - X)) = \text{Det}(x - X)$ as the matrix model description of an FZZT brane [33]. Since x describes the position of the brane, that is, the allowed places where open strings can end, it is natural to identify x with the target space coordinate. Since the Baker-Akhiezer function is an entire function, x runs over \mathbb{P}^1 . We can write formally

$$\text{Det}(x - X) \rightarrow D = \sum_i x^{N-i} (-1)^i \sum_{\sigma \in S_i} (-1)^\sigma \sigma \quad (2.58)$$

This is a universal formula which works for correlation functions of $\text{Det}(x - X)$ inside the delta functions as in (2.55). The lesson which emerges from equations (2.58) and (2.55) is that the operator which creates FZZT branes is *a fermionic condensate of worldsheet ramification points*. It would be interesting to clarify the connection between this remark and the interpretation of FZZT-branes as a condensate of long strings [34].

For the resolvent

$$R(x) = \text{Tr} \frac{1}{x - X} = \sum_{k=0}^{\infty} x^{-k-1} \text{Tr} X^k \quad (2.59)$$

we have

$$\langle R(x) \rangle_{\text{tr} X^2 + V} = \delta((R \circ e_{\circ}^{\hat{V}}) \mathbf{T} \mathbf{\Omega}) \quad (2.60)$$

where $R = \sum_k x^{-k-1} c_k$. The resolvent is a very useful auxiliary function used when determining the large N eigenvalue density. One can define a quadratic equation which determines the resolvent. This equation defines the spectral curve, which has a natural interpretation in terms of topological string theory on certain Calabi-Yau manifolds [35, 36]. The spectral curve can also be used to compute correlators at genus zero and higher genus [37].

It is interesting that the area dependence in the string theory of 2dYM [9] appears through exponentials such as $e^{AT_2^{(d)}}$, where $T_2^{(d)}$ is the sum of elements in the conjugacy class of simple transpositions in S_d . At each order in the expansion of the exponential, the product $(T_2^{(d)})^k$ is a product in the class algebra of a fixed symmetric group S_d . These products lead to counting problems with k simple branch points. For the 1-matrix model at hand we encounter the outer exponential of (2.50). In a sense the difference between the areas in string theory of 2dYM (generalized “areas” couple to higher branch points [14, 38]), which sums over different numbers of branch points, and the couplings of the string theory of the 1-matrix model, which is about three branch points but different ramification types, arises from the choice of exponentials in symmetric groups.

3 Feynman Graphs and the absolute Galois group

Traditionally we think of the Feynman graphs for matrix model correlators in terms of *double line diagrams*, following 't Hooft [39]. Equivalently we can use the language of *ribbon graphs*, where the propagators are single lines, but each vertex is equipped with a cyclic ordering of the edges (see for example [40]). In section 2 we have expressed correlators using triples of permutations (which multiply to one) of the kind that appear in counting branched covers with 3 branch points. This allows an immediate use of a theorem of Belyi to deduce an interesting connection to curves and maps defined over algebraic numbers (section (3.2)). Grothendieck exploited this theorem of Belyi to show that the absolute Galois group $\text{Gal}(\bar{\mathbb{Q}}/\mathbb{Q})$ acts on the equivalence classes of triples of permutations (Hurwitz-classes for

branched covers with 3 branch points). In his discussion, Grothendieck used the notion of Dessin D’Enfants (Dessins for short), which are yet another way to talk about ribbon graphs or double-line Feynman diagrams. The upshot is that “double-line Feynman diagrams of the 1-Matrix Model”, “Dessins ” , “ribbon graphs” , “triples of permutations” are all different descriptions of the same thing, and they admit an action of the absolute Galois group.

Having a precise characterization of Feynman diagrams in terms of triples of permutations allows us then to observe that the Galois group acts on Feynman graphs of the one-matrix model, or equivalently on the pairs (Σ_h, f) where Σ_h is the string worldsheet and f a holomorphic map to the target space \mathbb{P}^1 with 3 branch points. Most of the mathematical elements of this remark are found already in [40, 41], but have not been fully interpreted and exploited in the string theory literature. The current section explains, with concrete examples, the role of the Galois group in organising the Feynman graphs of the 1-Matrix model. In section 4, we will extend our considerations to multi-matrix models, where we are lead to introduce a new combinatoric object, colored-edge Dessins. In section 5 we will use these to find new results on invariants of the Galois action on ordinary Dessins.

3.1 3 Branch points : The Observable, The Wick contraction and the Product

The key result from the previous section (2.3) is that *any* correlator of the one matrix model, Gaussian or perturbed, can be written as a sum over maps from a Riemann surface to the sphere. The genus h of the Riemann surface determines the power of N , which is N^{2-2h} , at which it contributes. The map has three branch points with monodromies $\sigma, \gamma \in [2^n]$ and τ . The monodromy σ determines the observable whose correlator we are computing, γ is determined by the Wick contraction and τ is the product $\gamma^{-1}\sigma^{-1}$. Our goal in this section is to explore and develop the consequences of this observation. We will associate σ with the ramification over 0, γ with the ramification over 1 and τ with the ramification over ∞ . To reflect this in our notation we will sometimes refer to σ, γ, τ as $\sigma_0, \sigma_1, \sigma_\infty$.

3.2 Belyi’s theorem : From Three branch points to $\bar{\mathbb{Q}}$

Useful references for this section are [42, 43, 44]. In what follows we will consider algebraic number fields, which are field extensions of the field of rational numbers \mathbb{Q} . Thus, an algebraic number field is a field that contains \mathbb{Q} and has finite dimension when considered as a vector space over \mathbb{Q} . The field $\bar{\mathbb{Q}}$ obtained by adding all algebraic numbers to \mathbb{Q} will play an important role in what follows.

A classic theorem due to Weil states that a curve is defined over $\bar{\mathbb{Q}}$ if there exists a non-constant holomorphic function $f : \Sigma_h \rightarrow \mathbb{P}^1\mathbb{C}$ all of whose critical values lie in $\bar{\mathbb{Q}}$. Belyi’s theorem on algebraic curves states that given any algebraic curve defined over \mathbb{C} , it can be

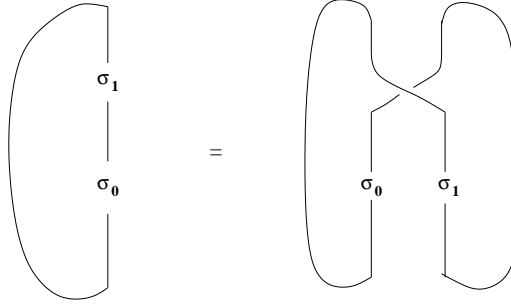


Figure 8: Tensor operator equality corresponding to cleaning of Belyi map

defined over $\bar{\mathbb{Q}}$ if and only if there exists a holomorphic function $f : \Sigma_h \rightarrow \mathbb{P}^1$ such that its branch points lie in the set $\{0, 1, \infty\}$. Following conventions in Belyi literature, we will use the notation $X = \Sigma_h$ and $\beta = f$. The pair (X, β) where X is a compact Riemann surface and $\beta : X \rightarrow \mathbb{P}^1$ is a holomorphic map unbranched outside the set $\{0, 1, \infty\}$, both defined over $\bar{\mathbb{Q}}$, is called a Belyi pair and we call β a Belyi function.

The inverse image under β of the closed interval $[0, 1]$ defines a Grothendieck Dessin (or just Dessin for short). The points in the preimage of 0 are marked with a black vertex and the points in the preimage of 1 are marked with a white vertex. Permutations σ_0, σ_1 can be assigned to Dessins by labelling the edges and going round the black and white vertices respectively (see for example the explanation in [44]).

A clean Belyi map is one which has all ramification orders equal to 2 over the point at 1. The Dessin corresponding to a clean Belyi map has exactly two edges for every preimage of 1. Given a general map α of Belyi type, we can get a new Belyi map β with $\beta = 4\alpha(1 - \alpha)$, such that β is a clean Belyi map. Recall from the previous subsection that since $\gamma \in [2^n]$, it is clear that it is the clean Belyi maps that arise as Feynman graphs in the 1-matrix model. The ramification orders above the point 0 are described by σ .

From the point of view of a Dessin, the process of cleaning amounts to converting the white vertices into black vertices and introducing white vertices in the middle of the edges joining the white vertices. If, with a labelling of the edges, $\sigma_0 \in S_d$ describes the permutation of edges around the black vertices, and $\sigma_1 \in S_d$ describes the permutation of the edges around the white vertices, then after the cleaning operation, $(\sigma_0 \circ \sigma_1) \in S_{2d}$ describes the permutation of the black vertices and a permutation which maps $\{1 \cdots d\}$ to $\{d+1, d+2, \dots, 2d\}$ pairwise, i.e the permutation with cycle decomposition $(1 \ d+1)(2 \ d+2) \cdots (d \ 2d)$, describes the permutation around the white vertices. In terms of tensor diagrammatics, sequences σ_0, σ_1 acting on $V^{\otimes d}$ have a trace given by the diagram on the left of Figure 8. The same trace can be described as a trace of something in $V^{\otimes 2d}$ by a simple diagrammatic manipulation, as in the right of Figure 8.

As a side-remark, consider the Dessin associated to a clean Belyi pair. After choosing a marking of the Dessins, the oriented cartographic group C_2^+ , an infinite discrete group,

permutes these marked Dessins. It is possible to prove that Dessins associated to a clean Belyi pair (which are also the Feynman graphs in the 1-matrix model) are in 1-1 correspondence with the conjugacy classes of subgroups of C_2^+ [42]. The generators of C_2^+ are ρ_0, ρ_1, ρ_2 with relations $\rho_1^2 = 1, \rho_0\rho_1\rho_2 = 1$. Thus, Feynman graphs are in 1-1 correspondence with conjugacy classes of subgroups of the Cartographic group.

3.3 $Gal(\bar{\mathbb{Q}}/\mathbb{Q})$ for organizing Feynman graphs

An important group in number theory, called the absolute Galois group $Gal(\bar{\mathbb{Q}}/\mathbb{Q})$, organizes all the key properties of the algebraic numbers. It is the group of all automorphisms of the algebraic closure $\bar{\mathbb{Q}}$ that fix \mathbb{Q} . By allowing the absolute Galois group to act on the numerical coefficients appearing in the Belyi pair, we get an action of the group on Dessins. The Galois group acts faithfully on Dessins². This means that the Galois group acts faithfully on the Feynman diagrams, and sets of Feynman diagrams can be assembled into Galois orbits. We have exploited the symmetric groups for organizing the Feynman graphs contributing to the Matrix model correlator. Now we are saying that the absolute Galois group can further be used to organize the Feynman graphs into orbits.

The correlator $\langle \mathcal{O}_{\sigma_0} \rangle$ in the the Gaussian 1-Matrix model is a sum over Hurwitz classes weighted by $1/|Autf|$. Choosing a multitrace operator is a choice of $[\sigma_0]$. Choosing a Wick contraction is a choice of a permutation σ_1 from the conjugacy class $[\sigma_1] = [2^n]$. Then we sum over $[\sigma_\infty]$ which runs over conjugacy classes that can appear in the product of permutations from $[\sigma_0]$ and $[\sigma_1]$. When computing the correlator of the gauge invariant operator, contributions are weighted by $\frac{1}{|Autf|}$ (see 2.21). It is known that the data $[\sigma_0], [\sigma_1], [\sigma_\infty], Autf$ are Galois invariants [45]. This means that every 1-point function $\langle \mathcal{O}_{\sigma_0} \rangle$ is a sum over Galois invariant data. The set of Hurwitz classes which share the above data can be one or many, and they can fit in one or more complete Galois orbits. When there are multiple orbits for fixed $[\sigma_0], [\sigma_1], [\sigma_\infty], Autf$, there will be a list of finite subgroups of $Gal(\bar{\mathbb{Q}}/\mathbb{Q})$ which will each act transitively on each orbit. In one of our examples of 3.4, this Galois group will be an S_3 acting as permutations of the three roots of (3.4).

It is worth noting that the Galois invariance of the conjugacy classes $[\sigma_0], [\sigma_1], [\sigma_\infty]$ is also useful in proving the finiteness of the length of the Galois orbit for any Dessin. There is a lot of mathematical interest in developing a complete list of Galois invariants which can be used to determine when a pair of Dessins are in the same orbit and when they are not [42, 43, 46, 47].

In the above, we have described the route from Feynman graphs to triples of permutations. Grothendieck relates these triples to Dessins. Now we explain how to obtain the Dessins directly from the Wick contractions without going through the triple of permutations: Each

²In fact, $Gal(\bar{\mathbb{Q}}/\mathbb{Q})$ acts faithfully on the set of genus 1 Dessins, on the set of genus 0 Dessins and even on the set of trees[42].

trace operator $\text{tr } X^k$ corresponds to a black vertex with k edges emerging from it, cyclically ordered using the orientation on a plane. Join the edges emerging from the vertices, in pairs, according to the Wick contractions. Insert a white vertex along every propagator and introduce extra handles to avoid intersections. The result is a clean Dessin.

We know how to get the Dessin from the Belyi pair: the Dessin is the inverse image of the closed interval $[0, 1]$ with points in the preimage of 1 marked with a white vertex and points in the preimage of 0 marked with a black vertex. It is possible to go in the other direction and obtain the Belyi pair from the Dessin [48, 44]. Start by placing a point within each closed region of the Dessin and label it as ∞ . Connect this new point to the black and white points forming the boundary of the region, connecting multiple times to the same black or white point if it appears multiple times on the boundary of the region. The result is a set of triangles each of which has three vertices, one labeled 0 (for the black point), one labeled 1 (for the white point) and ∞ (the new point). Each triangle is a half-plane. If the triangle has 0, 1, and ∞ in counterclockwise order it is an upper half-plane and if not, it is a lower half-plane. Adjacent pairs of triangles can now be glued together along the shared portion of their boundaries. The result is a Riemann surface. It can be mapped to the Riemann sphere by using the identity map within each half-plane so that we have indeed obtained a Belyi pair.

The role of $\text{Gal}(\bar{\mathbb{Q}}/\mathbb{Q})$ in organizing Feynman graphs of the 1-matrix model is rather different from the action of symmetries we are used to in quantum field theory. Usually we relate correlators of different observables, when the observables fall in representations of a symmetry group. Another good example are the Schwinger-Dyson equations in the 1-matrix model, which are a consequence of the invariance of the matrix integral under changes of variable. The Schwinger-Dyson equations relate the correlators of different observables to each other. In this case, the Galois group $\text{Gal}(\bar{\mathbb{Q}}/\mathbb{Q})$ relates different contributions to a fixed observable. Perhaps the MHV re-organization of Feynman diagrams [49] is a reasonable analogy to this organization, although we are not aware of a group which relates the set of different Feynman diagrams which are collected together in the MHV method.

3.4 Examples

The connections developed above can be made very concrete in the context of specific examples. For a sequence of observables in the Gaussian 1-matrix model, described by conjugacy classes $[\sigma_0]$ in S_{2n} , we will consider the class algebra multiplication $[\sigma_0] \cdot [2^n]$. For each $[\sigma_\infty]$ appearing in the product, we will consider

- The Hurwitz classes, their genus and automorphism group
- The size of the Galois orbit
- The Belyi pair

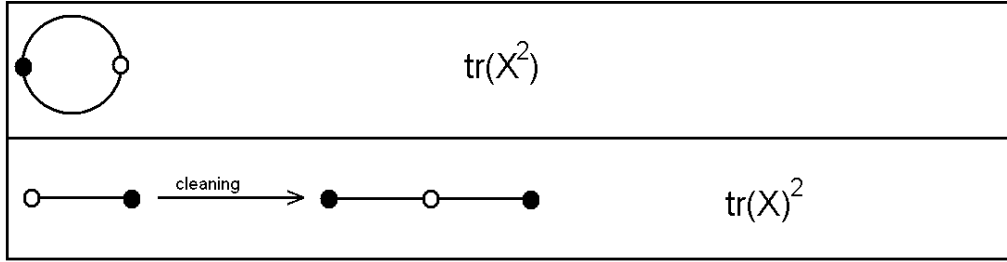


Figure 9: The Dessins corresponding to operators built using two matrices

- The field of definition

These choices deserve a few comments. The nature of the Galois orbit will provide insight into the symmetry which organizes the Feynman graphs. The field of definition is interesting, since its giving detailed information about the Belyi map itself. Related to fields of definition is the moduli field K which is the intersection of all the fields of definition [43]. The moduli field K is interesting because $\deg[K : \mathbb{Q}]$ is equal to the size of the orbit. In our examples, the need to distinguish K from the minimal field of definition will not be necessary.

- $\langle tr X^2 \rangle : [2] \cdot [2] = 2[1^2]$

There is a single Hurwitz class, a single ribbon graph corresponding to $[1^2]$. Since there is a one-to-one correspondence between ribbon graphs and Dessins, this immediately implies that the size of the Galois orbit has to be 1. Hence $\deg[K : \mathbb{Q}] = 1$, which means the field of definition is $K = \mathbb{Q}$. $|Aut(f)| = 2$. The Belyi map corresponding to this observable is

$$w = \frac{z^2}{z - \frac{1}{4}} \quad (3.1)$$

The corresponding Dessin is given in Figure 9.

- $\langle (tr X)^2 \rangle : [1^2] \cdot [2] = [2]$

There is a single Hurwitz class, a single ribbon graph which immediately implies that the size of the Galois orbit has to be 1. Hence $\deg[K : \mathbb{Q}] = 1$, which again means the field of definition is $K = \mathbb{Q}$. $|Aut(f)| = 2$. From Figure 9 it is clear that the Dessin for this observable can be obtained by cleaning the Dessin whose Belyi map is $w = z$, which gives

$$w = 4z(1 - z) \quad (3.2)$$

- $\langle tr X^4 \rangle : [4] \cdot [2^2] = 2[2 \ 1^2] + [4]$

There are two Hurwitz classes, one for $[2 \ 1^2]$ and one for $[4]$. One corresponds to a map

from the sphere to the sphere and one to a map from the torus to the sphere. Since genus is a Galois invariant, this correlator gets contributions from two Galois orbits each of which have size 1. Thus, the field of definition for both is again $K = \mathbb{Q}$. The map for the Dessin of genus zero is

$$w = \frac{(z - \frac{3}{2})^4}{(z - 1)(z - 2)} \quad (3.3)$$

The two poles in the Belyi function are needed because each closed loop in the Dessin contains the point $w = \infty$. These are the new points that we added in order to obtain the Belyi pair from the Dessin in section 3.3. This Dessin is given in Figure 10. A model for the genus 1 Dessin is more involved, because we need both a model for the map and for the torus. The fact that there is a single Feynman diagram appearing in the orbit implies that the Belyi pair will have all coefficients in \mathbb{Q} . The Belyi curve (worldsheet of torus topology) is defined by the

$$y^2 = x^3 - x$$

and the Belyi map is

$$w = x^2$$

The reader can readily verify that, as $x \rightarrow 0$, we can choose local coordinates $w = \epsilon_1$ on the target and ϵ_2 on the worldsheet ($y = \epsilon_2, x = -\epsilon_2^2$) so that $\epsilon_1 = \epsilon_2^4$ as required for a ramification point described by a 4-cycle. For $w = 1$, we have worldsheet points $(x = 1, y = 0), (x = -1, y = 0)$. Take the first : a local coordinate on the worldsheet is ϵ_2 with $(x = 1 + \frac{\epsilon_2^2}{2}, y = \epsilon_2)$. On the target a local coordinate is $(w - 1) = \epsilon_1$ and locally the map is $\epsilon_1 = \epsilon_2^2$ as required for a simple ramification point. The same argument holds at $(x = -1, y = 0)$ so that we have ramification profile $[2^2]$ over $w = 1$. Near $w = \infty$, we have $w = x^2, y^2 = x^3$. We can choose local coordinate ϵ_1 on the target with $w = \frac{1}{\epsilon_1}$ and ϵ_2 on the worldsheet with $(y = \frac{1}{\epsilon_2^3}, x = \frac{1}{\epsilon_2^2})$, so that $\epsilon_1 = \epsilon_2^4$ as required for ramification profile $[4]$ over $w = \infty$.

- $\langle tr X^3 tr X \rangle : [3\ 1] \cdot [2^2] = [3\ 1]$

There is a single Hurwitz class and hence a single element in the Galois orbit so that again $K = \mathbb{Q}$. The Belyi map of this Dessin is

$$w = \frac{(z + \frac{13}{4})(z + \frac{5}{4})^3}{z + 1}$$

We can easily see that $z = \frac{-13}{4}$ has image $w = 0$ and no ramification, while $z = \frac{-5}{4}$ also mapping to $w = 0$ is a third order zero, so the ramification profile over $w = 1$ is $[3\ 1]$. Points $z = \frac{-7}{4} \pm \frac{\sqrt{3}}{2}$ on the worldsheet map to $w = 1$ and each is a second order zero of $w - 1$ thus describing ramification profile $[2^2]$ over $w = 1$. The points $z = -1$ and $z = \infty$ map to $w = \infty$. While $z = 1$ is a simple pole, the large z, w behaviour is $w \sim z^3$, so that $w = \infty$ has a ramification profile $[3\ 1]$.

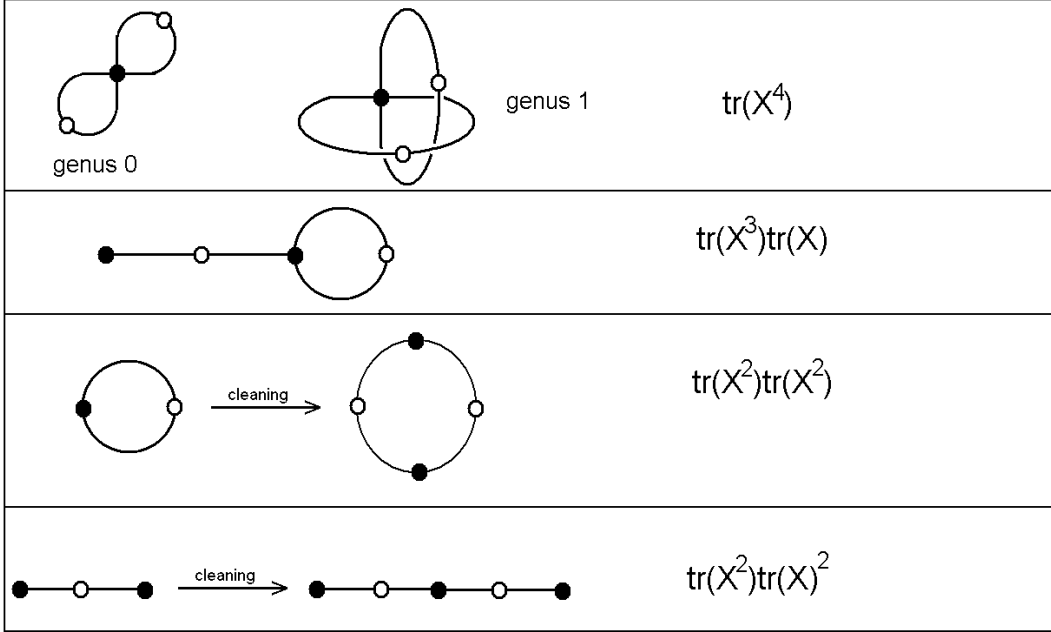


Figure 10: The Dessins corresponding to operators built using four matrices

- $\langle (\text{tr} X^2)^2 \rangle : [2^2] \cdot [2^2] = 3[1^4] + 2[2^2]$

The contribution coming from $[1^4]$ is disconnected and hence is not considered. There is a single Hurwitz class corresponding to $[2^2]$, a single element in the Galois orbit and so $K = \mathbb{Q}$. The Belyi map of the Dessin can be obtained by cleaning from the $\text{Tr}(X^2)$ Belyi map 3.1, which gives

$$w = \frac{4z^2(z - \frac{1}{4} - z^2)}{(z - \frac{1}{4})^2}$$

- $\langle \text{tr} X \text{tr} X \text{tr} X^2 \rangle : [2^1 1^2] \cdot [2^2] = [2^1 1^2] + 2[4]$

The contribution corresponding to $[2^1 1^2]$ is disconnected and hence not considered. There is a single Hurwitz class corresponding to $[4]$. This class which is related to Chebyshev polynomials, have a chain Dessin [43]. There is again a single element in the Galois orbit so that again $K = \mathbb{Q}$. The Belyi map of the Dessin can be obtained by cleaning from the $(\text{Tr} X)^2$ Belyi map (3.2)

$$w = 16z(1 - z)(1 - 2z)^2$$

- $\langle (\text{tr} X)^4 \rangle$:

All contributions are disconnected.

- The (single) connected Feynman diagram contributing to the correlator

$$\langle (\text{Tr} X^k)(\text{Tr} X)^k \rangle$$

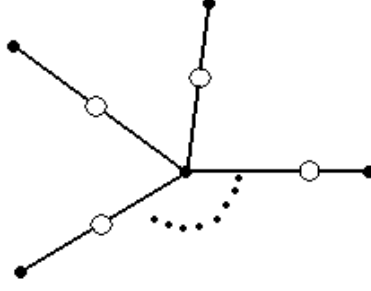


Figure 11: A Dessin for the connected piece of $\langle (\text{Tr } X^k)(\text{Tr } X)^k \rangle$.

is given by the Dessin in Figure 11. The Belyi function for this flower is[50]

$$w = (1 + x^k)^2$$

The field of definition is equal to the moduli field is equal to \mathbb{Q} . Thus, these belong to a Galois orbit of length 1. Further, this Dessin is the only Dessin that arises in the connected correlator so that this connected correlator gets its complete contribution from a single Galois orbit. By applying the cleaning map to these we would get Dessins that give one of many contribution to correlators of the form

$$(\text{Tr } X^k)(\text{Tr } X^2)^k(\text{Tr } X)^k$$

Thus, for $k > 2$ all of these correlators we get contributions from more than one Galois orbit. Consider the case $k = 3$. We have $[\sigma_0] = [32^3 1^3], \sigma_1 = [2^6]$. There are a total of four connected diagrams associated with the conjugacy class made of one cycle of length 12. One of them is defined over rationals as above and lies alone in a Galois orbit. The other three lie in a single orbit; they correspond to the cleaned versions of the Dessins shown in Figure 12. The Belyi functions for the Dessins of Figure 12 take the form

$$w = z^3(z - a_1)(z - a_2)^2$$

To fix a_1 and a_2 following the method of [43] one needs to pick a root of

$$25\alpha^3 - 12\alpha - 24\alpha - 16 = 0 \tag{3.4}$$

Each root corresponds to a particular Dessin. Given α compute

$$b = \frac{5 + 4\alpha - \sqrt{(5 + 4\alpha)^2 - 62\alpha}}{12}$$

and (the six possible roots for a_1 all give rotated versions of the single Dessin)

$$a_1 = \left(\frac{1}{b^3(b-1)(b-\alpha)} \right)^{\frac{1}{6}}$$

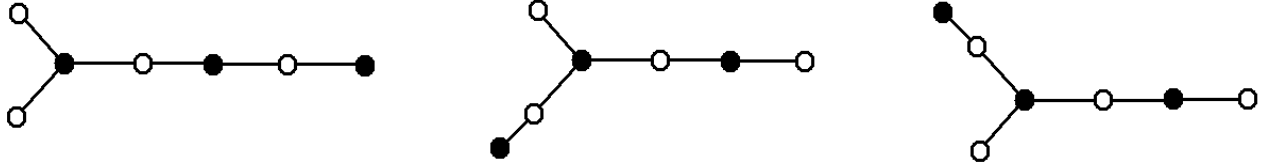


Figure 12: The Dessins shown belong to a single Galois orbit.

$$a_2 = \alpha a_1$$

The field generated by the defining polynomial (3.4) has discriminant $-5038848 = -2^8 3^9 [51]$. This is not a perfect square which tells us that the Galois group of this field is $S_3 [52]$.

- There is another interesting example of an operator which receives contributions from Dessins belonging to more than one orbit. The Leila Flowers are a pair of genus zero Dessins (in fact trees) which can be described by permutations

$$\begin{aligned} [\sigma_0] &= (1)^{15}(5) \\ [\sigma_1] &= (2)(3)(4)(5)(6) \\ [\tau] &= (20) \end{aligned} \tag{3.5}$$

By cleaning (See Figure 17) we have genus zero Dessins with

$$\begin{aligned} [\Sigma_0] &= (1)^{15}(2)(3)(4)(5)^2(6) \\ [\Sigma_1] &= (2)^{20} \\ [\tau] &= (40) \end{aligned} \tag{3.6}$$

Hence there are at least 2 distinct Galois orbits contributing to the connected piece of

$$\langle (tr(X))^{15} tr(X^2) tr(X^3) tr(X^4) (tr(X^5))^2 tr(X^6) \rangle \tag{3.7}$$

3.5 Belyi pairs and square Strebel differentials

Zapponi [53, 54] describes how to go from a Dessin to a Ribbon-graph which is the critical graph of a quadratic differential ω . The Dessin is the inverse image of $[0, 1]$. The critical graph of the quadratic differential is the inverse image of the unit circle. For a quadratic differential to correspond to a Belyi-pair, its ribbon graph must be bi-colorable. This is equivalent to requiring that the quadratic differential is a square of a holomorphic differential. From the Belyi data the holomorphic differential is $\frac{d\beta}{\beta}$. The vertices of the critical graph correspond to the ramification points over 1. For clean Belyi maps, these $d\beta$ have a zero of order 1, hence ω has a zero of order 2 and consequently the critical graph has valency 4. For the curve defined over $\bar{\mathbb{Q}}$, the lengths are all 1 [55]. These facts constrain the places of $\mathcal{M}_{g,n}$

which correspond to clean Belyi maps of degree $2n$. Since the quadratic differentials and their critical graphs give a cell decomposition of $\mathcal{M}_{g,n}$ as well as a combinatoric description of Mumford Morita-classes [56], these facts should be useful in developing a combinatoric derivation of ELSV type formulae [57] in terms of Mumford Morita-classes for the Hurwitz numbers we have derived.

It is interesting that Strebel differentials, and the Galois action on Dessins have been studied in a physics context before in connection with Seiberg-Witten theory [58]. Strebel differentials also a prominent role in the programme of [59].

3.6 Topological string theory on \mathbb{P}^1

We have seen that the 1-matrix model has an interpretation as a string theory with a \mathbb{P}^1 target space. It is then natural to look for a topological string theory on \mathbb{P}^1 which reproduces the correlators of the matrix model. A connection between topological σ -models and large N -matrix integrals has been established in [60]. This work provides an explicit matrix model which reproduces the topological σ -model (A-model) coupled to gravity on \mathbb{P}^1 . The observables of the topological σ -model come from the de Rahm classes of the target manifold. For \mathbb{P}^1 there are two de Rahm classes, the identity and the Kähler class. Denote the corresponding physical observables P and Q . Further, because the topological σ -model is coupled to gravity, new observables given by gravitational descendents of P and Q can be constructed. Any of these observables can be added as a term in the action with a coupling t_P (t_Q) for P (Q), and with a coupling $t_{n,P}$ ($t_{n,Q}$) for the n th descendant of P (Q) respectively. The corresponding matrix model is

$$Z = \int dM e^{-\text{Tr}V(M)}$$

where

$$\text{Tr} V(M) = -2\text{Tr} M(\log M - 1) + \sum_{n=1} 2t_{n,P} \text{Tr} M^n (\log M - c_n) + \sum_{n=1} \frac{1}{n} t_{n-1,Q} \text{Tr} M^n$$

$$c_0 = 0 \quad c_n = \sum_{j=1}^n \frac{1}{j}$$

The matrix M is an $N^* \times N^*$ matrix with $N^* = Nt_{0,P}$. To get the Gaussian matrix model we should choose $t_{1,P} = 1$, $t_{1,Q} = 1$ and set all other couplings equal to zero. Since the perturbation is being chosen to cancel the logarithmic term, this may well be a subtle limit of the model.

One could also consider a more direct route to constructing the relevant topological string theory on \mathbb{P}^1 . It is shown in [53] how to obtain Strebel graphs from Dessins. These Strebel graphs are not the most general. Rather they have the property that they are related to quadratic differentials which are squares of ordinary holomorphic differentials. In fact, in

terms of the Belyi map, we have $\omega_{zz} = \frac{\partial_z f}{f} \frac{\partial_z f}{f}$. Topological string constructions can be designed to localize on the solution sets of appropriate equations. This equation should form the basis of a topological string construction with \mathbb{P}^1 target where the constraint of three branch points is automatically included.

Some insights on the string dual of 2dYM, which has a string theory interpretation in terms of two-dimensional target spaces Σ_G , have been obtained by developing an interpretation in terms of a six-dimensional Calabi-Yau target space which are bundles over Σ_G [63]. It would be interesting in the case of the string dual of the Hermitian Matrix model to explore if a six-dimensional target space interpretation can provide a natural home for the \mathbb{P}^1 with three branch points discussed here.

4 Multi-Matrix models and colored-edge Dessins

4.1 Multi-Matrix models

Consider the Gaussian 2-matrix model and a multi-matrix operator $tr(\sigma X^{\otimes 2n_1} \otimes Y^{\otimes 2n_2})$. The correlator is given by

$$\begin{aligned} \langle tr(\sigma X^{\otimes 2n_1} \otimes Y^{\otimes 2n_2}) \rangle &= \sum_{\gamma_1 \in [2n_1]} \sum_{\gamma_2 \in [2n_2]} tr_{2n}(\sigma \gamma_1 \circ \gamma_2) \\ &= \sum_{\tau \in S_{2n}} \sum_{\gamma_1, \gamma_2} \delta(\sigma(\gamma_1 \circ \gamma_2)\tau) N^{C_\tau} \end{aligned} \quad (4.1)$$

The choice of an operator, say $trXYtrXY$, chooses a coloring of the cyclically ordered edges coming out of a black vertex (associated with σ_0 in Belyi literature conventions, here σ). The choice of a contraction gives a clean Dessin, equipped with the additional data of a coloring of the edges. Any open circle (associated with σ_1 in Belyi literature conventions, here $\sigma_1 = \gamma_1 \circ \gamma_2$) has 2-edges of the same color, which form the propagator in the matrix theory language. We can think of X and Y propagators as having different colors. For an earlier use of related ideas see [64].

In the case of the 1-matrix model, we normalized the 1-point functions by introducing $\frac{||[\sigma]||}{(2n)!}$. Here $2n_1 + 2n_2 = 2n$ and the natural normalization factor is

$$\frac{||[\sigma]_{(2n_1, 2n_2)}||}{(2n_1)!(2n_2)!} \quad (4.2)$$

where $[\sigma]_{(2n_1, 2n_2)}$ is the set of permutations in S_{2n} related to σ by conjugation with elements in $S_{2n_1} \times S_{2n_2}$. This is analogous to the fact that $[\sigma]$ was the set of elements related to σ by conjugation in S_{2n} , equivalently the elements in the same conjugacy class as σ or elements with same cycle structure. A natural guess now is that the answer will be related to $Aut(D_{col})$, the automorphism group of the colored Dessin. It is clear that the colored Dessin

D_{col} gives a clean Dessin D of usual type (familiar from Belyi literature) by forgetting the colors. This has $Aut(D)$ which is the same as the $Aut(f)$, the automorphism of the holomorphic map. As a step towards the definition of $Aut(D_{col})$, note that two colored Dessins are equivalent when they are related by permutations in $S_{2n_1} \times S_{2n_2}$. We are lead to

$$Aut(D_{col}) = Aut(D) \cap (S_{2n_1} \times S_{2n_2}) \quad (4.3)$$

Both $Aut(D)$ and $(S_{2n_1} \times S_{2n_2})$ are subgroups of S_{2n} and the intersection is a subgroup. This symmetry appears in the appropriately normalized correlator

$$\begin{aligned} \frac{|[\sigma]_{(2n_1, 2n_2)}|}{(2n_1)!(2n_2)!} N^{C_\sigma - n} \langle tr(\sigma X^{\otimes 2n_1} \otimes Y^{\otimes 2n_2}) \rangle &= \sum_{\sigma \in [\sigma]_{2n_1, 2n_2}} \sum_{\tau, \gamma_1, \gamma_2} \frac{N^{\chi(D)}}{(2n_1)!(2n_2)!} \delta(\sigma(\gamma_1 \otimes \gamma_2)\tau) \\ &= \sum_{D_{col}} \frac{N^{\chi(D)}}{|Aut(D_{col})|} \end{aligned} \quad (4.4)$$

The last line follows from a general fact about group actions. In this case there is an action by conjugation of $S_{2n_1} \times S_{2n_2}$ on the permutations solving the delta function and the multiplicity of equivalence classes is given by the order of the cosets $\frac{(2n_1)!(2n_2)!}{|Aut(D_{col})|}$

The remark of section 2.4 generalizes to the colored case.

$$N^{C_\sigma - n} \langle tr(\sigma X^{\otimes 2n_1} \otimes Y^{\otimes 2n_2}) \rangle = \sum_{[D_{col}(\sigma)]} \frac{|Aut_{2n_1, 2n_2}(\sigma)|}{|Aut(D_{col})|} N^{\chi(D)} \quad (4.5)$$

The $Aut_{2n_1, 2n_2}(\sigma)$ is the group of permutations in $S_{2n_1} \times S_{2n_2}$ which leaves invariant $\sigma \in S_{2n}$

$$|Aut_{2n_1, 2n_2}(\sigma)| = \frac{(2n_1)!(2n_2)!}{|[\sigma]_{2n_1, 2n_2}|} \quad (4.6)$$

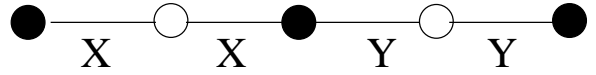
The ratio $\frac{|Aut_{2n_1, 2n_2}(\sigma)|}{|Aut(D_{col})|}$ is integral because $Aut(D_{col})$ is the intersection in $S_{2n_1} \times S_{2n_2}$ of $Aut_{2n_1, 2n_2}(\sigma)$ and $\gamma_1 \circ \gamma_2 \in ([2^{n_1}], [2^{n_2}])$. Hence it is a subgroup of $Aut_{2n_1, 2n_2}(\sigma)$. The ratio is the number of Wick contractions of $tr(\sigma(X \otimes Y))$ which give the colored-Dessin-equivalence class D_{col} . As before we also deduce the integrality of

$$\frac{2^{n_1+n_2} n_1! n_2!}{Sym([\sigma]_{2n_1, 2n_2})} \langle tr(\sigma X \otimes Y) \rangle \quad (4.7)$$

Note that *the set* of D_{col} for a given D is clearly a property of the Hurwitz-class, i.e of the conjugacy class of (σ_0, σ_1) under simultaneous conjugation by S_{2n} , hence its a property of an equivalence class of holomorphic maps. This remark will be exploited in section 5 to build Galois invariants of the Hurwitz class.

4.2 Colored Dessins, permutation triples and subgroups of S_{2n}

In the classic case we have the correspondence between



**EQUIVALENT
COLORED-EDGE DESSINS**

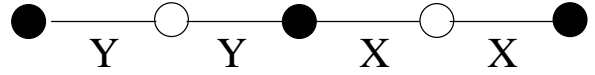


Figure 13: Colored Dessins in the same equivalence class

- Triples of permutations $\sigma_0, \sigma_1, \sigma_\infty$ in S_{2n} obeying $\sigma_0\sigma_1\sigma_\infty = 1$, up to equivalence under simultaneous conjugation in S_{2n} . Further permutation the σ_1 belongs to the conjugacy class $[\sigma_1] = [2^n]$.
- Clean Dessins d’Enfants which are graphs with alternating black and white vertices. The cyclic order for the edges at each vertex is part of the data of the graph. The white vertices have valency 2.

This correspondence implies that the automorphism of a triple is a symmetry of the Dessin. There is more we could add to this list of remarkable equivalences, including Hurwitz classes and Belyi-pairs of (X, β) defined over $\bar{\mathbb{Q}}$. To motivate our generalization, the above list is rich enough.

The above list generalizes to colored Dessins as follows

- Triples of permutations $\sigma_0, \sigma_1, \sigma_\infty$ with $\sigma_0 \in S_{2n_1}$, $[\sigma_1] \in [2^{n_1}, 2^{n_2}]$ in an $S_{2n_1} \times S_{2n_2}$ subgroup of S_{2n} obeying $\sigma_0\sigma_1\sigma_2 = 1$ up to equivalence under simultaneous conjugation in $S_{2n_1} \times S_{2n_2}$.
- Clean Dessins d’Enfants which are again graphs with alternating black and white vertices. The white vertices again have valency 2. In the colored Dessin, the edges can be red or blue. The edges incident on a white vertex are both red or both blue. The edges ending on a black vertex can have any color.

Automorphisms of the colored Dessin defined as conjugations in $S_{2n_1} \times S_{2n_2}$ which leave the triple fixed, coincide with the symmetry group of the colored Dessins.

We have given formal definitions of equivalence of the colored Dessins. In simple examples, this reduces to fairly obvious-looking equivalences. Two simple colored Dessins which are in the same equivalence class, are shown in Figure 13.

The following question is natural : What continuum object does a choice of D_{col} correspond to ? We will develop two related answers to this question. One is that a choice of D_{col}

is a pair consisting of (f, s) , a holomorphic map from a Riemann surface to \mathbb{P}^1 with branch points at $0, 1, \infty$ and a section s of a skyscraper sheaf on the Riemann surface. The second answer is that the colored Dessins define sheaves over Hurwitz space.

4.3 Coloring edges to coloring vertices

The Dessins that arise as Feynman diagrams of the Hermitian matrix model are *clean* Dessins. Each propagator is a pair of edges which are joined at a white vertex. These white vertices are inverse images of 1. Coloring the propagators is equivalent to coloring the white vertices instead and leaving the edges uncolored. Each Dessin determines a Riemann surface and an equivalence class of maps from the Riemann surface to \mathbb{P}^1 with three fixed branch points, chosen to be at $0, 1, \infty$. Recall that the white vertices correspond to inverse images of 1, which are ramification points of order 2. Each colored Dessin associates colors to these ramification points. This can be described in terms of skyscraper sheaves on the worldsheet, localised at the ramification points above 1, which associate the set of colors to these points. (We have found [61] to be a useful reference on the basics of sheaves we need for this discussion). Choosing a coloring is a choice of sections of the skyscraper sheaves. The Automorphism group $AutD_{col}$ can then be equated to $Aut(f, s)$ which is the automorphism of the pair consisting of the map from the worldsheet with simple ramification points above 1, along with a coloring of the ramification points. For the Dessins corresponding to the map f , the automorphisms are just maps ϕ obeying $f \circ \phi = f$. Such maps ϕ have to map the set of ramification points above 1 back to itself. To define $Aut(f, s)$ we also require that ϕ preserves the color at the ramification points. So we can say that

$$\frac{|[\sigma]_{(2n_1, 2n_2)}|}{(2n_1)!(2n_2)!} N^{C_{\sigma}-n} \langle tr(\sigma X^{\otimes 2n_1} \otimes Y^{\otimes 2n_2}) \rangle = \sum_{D_{col}} \frac{N^{\chi(D)}}{|Aut(D_{col})|} = \sum_{(f,s)} \frac{N^{\chi(D)}}{|Aut(f, s)|} \quad (4.8)$$

4.4 Sheaves of colored Dessins over Hurwitz space

Consider the Hurwitz space with 3 branch points at $0, 1, \infty$ on \mathbb{P}^1 . Consider small non-overlapping open discs drawn on the \mathbb{P}^1 . If we let the branch points move over their respective discs, there is a 3-complex dimensional subspace of Hurwitz space. The S_d equivalence classes of triples $[\sigma_0, \sigma_1, \sigma_\infty]$ describe different strata of Hurwitz space. Each of these strata is associated to a Dessin corresponding to $[\sigma_0, \sigma_1, \sigma_\infty]$. For our current applications we are interested in strata where $d = 2n$ and $[\sigma_1] = [2^n]$. For each choice of a positive integer k , we can consider colorings of the Dessins with k -colors, where we can further specify a partition of n of length k , i.e $n = n_1 + n_2 + \dots + n_k$. For each $(k, \vec{n} = (n_1, \dots, n_k))$, we have a set of equivalence classes of colored Dessins. Equivalently, as explained above we have the pairs (f, s) . We can define a sheaf over the set of Grothendieck Dessins by associating to each Dessin the set of equivalence classes of colorings of that Dessin. Since strata of Hurwitz space map to Dessins, we can pull back the sheaf of colored Dessins to

the open three-dimensional regions of Hurwitz space described above. This gives one answer to the question of the continuum interpretation of the colored Dessins. They are related to sheaves over Hurwitz space. We leave a more detailed and general discussion of such sheaves to the future, including the questions of how to extend the definition to compactified Hurwitz spaces where branch points are allowed to collide, Dessins degenerate and non-trivial restriction maps of sets of colored Dessins arise.

4.5 Hurwitz space and String theory for multi-matrix models

In section 2 we developed an interpretation of the one-matrix model at generic couplings in terms of a topological string theory which localizes on the Hurwitz space of holomorphic maps with three branch points on \mathbb{P}^1 target space.

In this section we have shown that the Hurwitz spaces for \mathbb{P}^1 target and 3 branch points continue to provide a string theory interpretation for multi-matrix models at generic couplings. Now it is a string theory related to sheaves over Hurwitz space.

It would be interesting to develop a more physical approach to this string theory, e.g as topological sigma model coupled to 2D gravity, or as some topological WZW CFT coupled to 2D gravity, perhaps along the lines of [62] where a physical set-up for intersection theory for bundles over $\mathcal{M}_{g,n}$ is described.

5 Colored-edge Dessins as a tool for Galois invariants

In the following we will refer to Grothendieck Dessins (ribbon graphs) as Dessins for short. We will use the abbreviations CEDs for colored-edge Dessins and MMOs for multi-matrix operators.³

5.1 From Dessin to list of colored-Dessins and list of multi-matrix operators

We showed in section 4 that the 1-point function of a multi-trace operator in multi-matrix theory is obtained by summing over certain triples of permutations which correspond to colored-edge Dessins (CEDs). These CEDs project to ordinary Dessins with black and white vertices by forgetting the edge-colorings. A simple example illustrating the concept of color-forgetting projection map from the set of equivalence classes of colored Dessins to ordinary Dessins is given in Figure 14.

We have labeled the colors as X, Y . Since the correlator of a given multi-matrix operator is a sum over colored-edge Dessins, multiple CEDs are associated to a single multi-matrix

³We apologize to readers who hate acronyms and appeal to their concern for the trees we save.

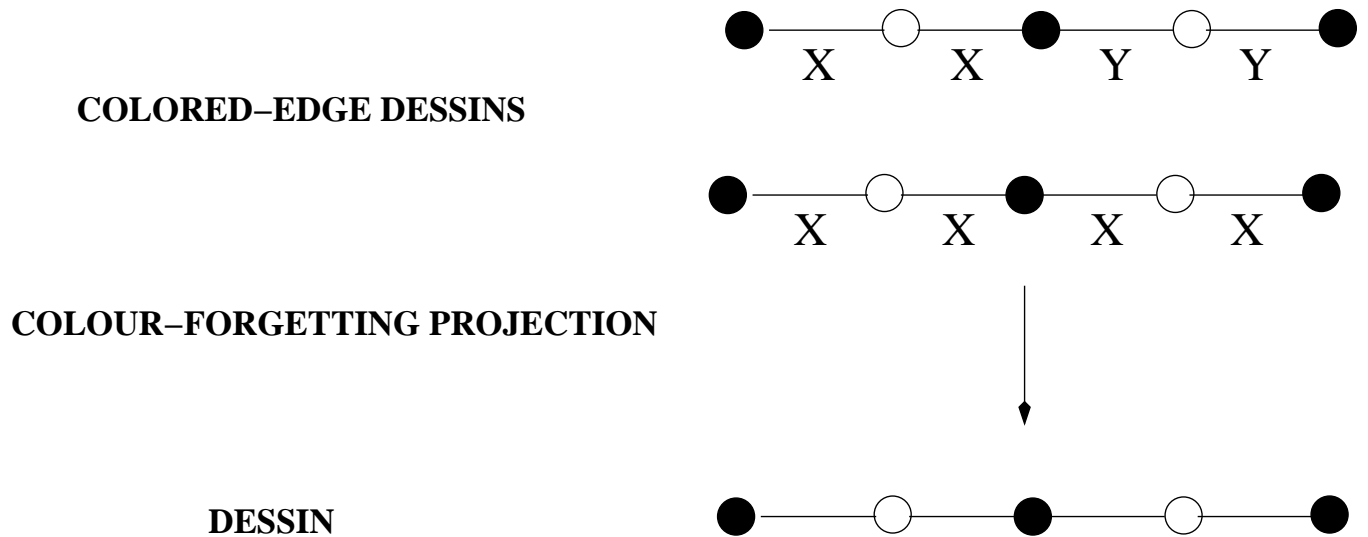


Figure 14: Equivalence classes of colored Dessins and projection to Dessin

operator (MMO). Forgetting the coloring gives an ordinary Dessin. We will show that the set of Dessins associated to a multi-matrix operator in this way do not form complete Galois orbits, unlike the case of the one-matrix model.

One can also associate a list of MMOs with a Dessin. For a fixed Dessin there is list of MMOs receiving contributions from the colorings of that Dessin, in other words, from the set of colored Dessins which project to the given Dessin.

The two-color-Dessin in Figure 14 arises when we consider the one-point function of $\text{tr}X\text{tr}Y\text{tr}XY$ in the Gaussian 2-matrix model. The fact that one black vertex has a single incident edge labeled with a single X , another black vertex has a single incident edge labeled with a single Y , and the middle black vertex has two incident edges labeled X, Y , reflect the structure of the operator. Colored Dessins, like ordinary Dessins, come equipped with a cyclic order at each vertex. This corresponds to the cyclic property of traces. The one-color Dessin in Figure 14 arises from considering the correlator of $(\text{tr}X)^2(\text{tr}X^2)$ in the Gaussian 1-matrix model. So we can associate, to the uncolored Dessin in the figure, two distinct MMOs, namely $(\text{tr}X)^2(\text{tr}X^2)$ and $\text{tr}X\text{tr}Y\text{tr}XY$. We will explain shortly how these lists of colored Dessins or lists of MMOs provide combinatoric Galois invariants.

A general Dessin where the white vertices do not all have exactly two incident edges, can as discussed in section (3.2) be converted into a clean Dessin by turning the white vertices into black vertices, and introducing white vertices in the middle of the existing edges. In the Galois theory literature, one performs this operation to define the *cartographic group* of a Dessin, which is a Galois invariant. We can also use this procedure of cleaning to associate to a Dessin combinatoric Galois invariants related to lists of CEDs or lists of MMOs.

We will describe a convenient way to generate lists of possible MMOs for a given Dessin

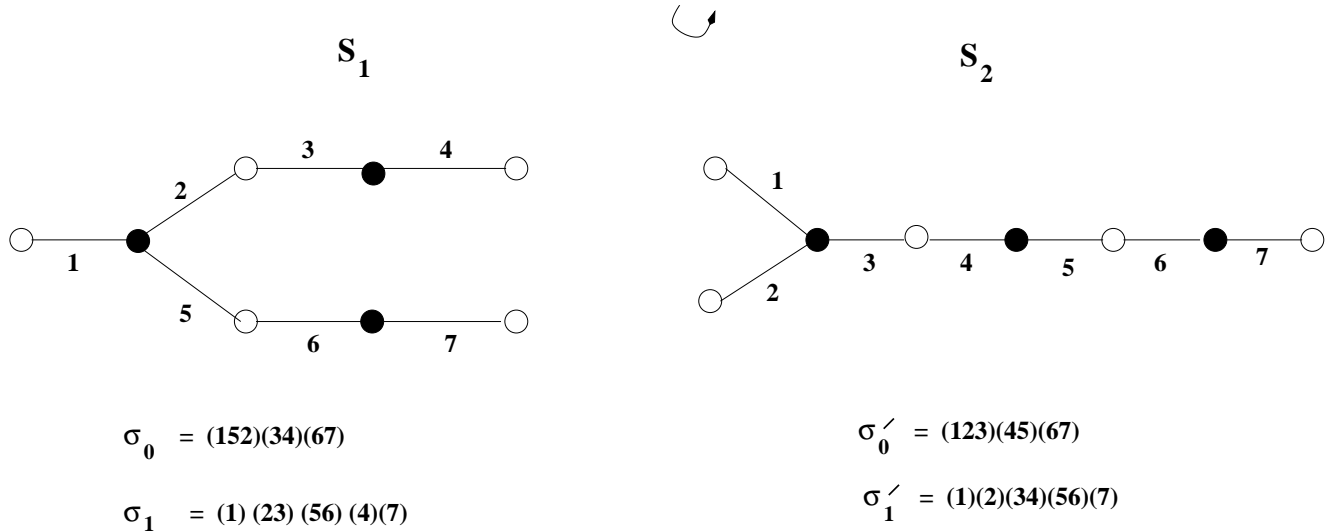


Figure 15: Two distinct Dessins with same cycle structure for permutations

with a given number of different matrix types, which can be done with a computer program⁴. For concreteness, we will describe the construction with the aid of an example. Take two Dessins as in Figure 15 which can be described by permutations as in the Figure. For the Dessin S_1 we have two permutations σ_0, σ_1 which can be read off by going round the black and white vertices respectively, in the orientation indicated. The same procedure produces a pair of permutations σ'_0, σ'_1 for the Dessin S_2 . The cycle structures of the (σ_0, σ_1) are the same as (σ'_0, σ'_1) but there is no permutation which can simultaneously conjugate the first pair to the second. So these are inequivalent Dessins. They are not clean Dessins. After applying the cleaning procedure, the cleaned version of S_1 is described by permutations

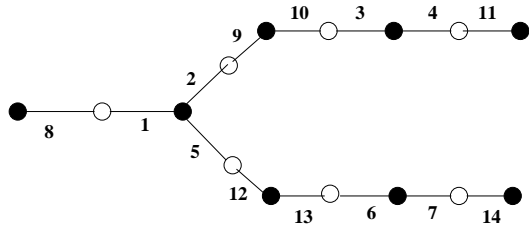
$$\begin{aligned} \Sigma_0 &= (152)(34)(67)(8)(9, 10)(11)(12, 13)(14) \\ \Sigma_1 &= (1, 8)(2, 9)(3, 10)(4, 11)(5, 12)(6, 13)(7, 14) \end{aligned} \quad (5.1)$$

The permutation Σ_0 is written down by composing σ_0 with a shifted version of σ_1 (see Figure 16). The cleaned version of S_2 is described by permutations

$$\begin{aligned} \Sigma'_0 &= (123)(45)(67)(8)(9)(10, 11)(12, 13)(14) \\ \Sigma'_1 &= (1, 8)(2, 9)(3, 10)(4, 11)(5, 12)(6, 13)(7, 14) \end{aligned} \quad (5.2)$$

To list the MMOs associated with these clean Dessins, proceed as follows. Fix a number of matrix types, say for example 2, i.e we are looking at X, Y . Fix the number of each matrix type, say $2n_1 = 10$ X 's and $2n_2 = 4$ Y 's. There are $\frac{n!}{n_1!n_2!} = \frac{7!}{5!2!}$ ways of distributing X, Y among $1, \dots, 7$. Each of these choices leads to a multi-matrix operator. By scanning this list we can get all the possible MMOs for two matrix types whose correlators in the 2-matrix model receive contributions from colored versions of each Dessin.

⁴code written in SAGE available from authors if desired



$$\Sigma_0 = (152)(34)(67)(8)(9,10)(11)(12,13)(14)$$

$$\Sigma_1 = (1,8)(2,9)(3,10)(4,11)(5,12)(6,13)(7,14)$$

Figure 16: Cleaned version of S_1 and permutations

It is known that S_0 and S_1 are in the same Galois orbit (see page 90-91 of [43] and [65]) In the above case, we see that the operator $(Y^2X)(YX)^2(X^2)^2(X)^3$ appears in the list for the cleaned version of S_1 but not in the cleaned version of S_2 . Its appearance in the cleaned version of S_1 arises by associating colors as $(2, 9) \rightarrow Y$, $(5, 12) \rightarrow Y$ and remaining pairs of edges in cleaned S_1 as X .

This example illustrates an important point, which was a priori not obvious to us. In the case of the Gaussian 1-matrix model with matrix X , an operator with non-zero 1-point function has $2n$ copies of X . The different ways of tracing are described by permutations $\sigma_0 \in S_{2n}$. Different elements in the conjugacy class $[\sigma_0]$ give the same operator. The computation of its correlator involves a sum over all permutations σ_1 in the conjugacy class with n cycles of length 2. This sum includes all possible Dessins with the specified conjugacy classes of $[\sigma_0], [\sigma_1]$. Two Dessin in the same Galois orbit necessarily have the same $[\sigma_0], [\sigma_1]$. This means that correlators in the 1-matrix model sum over complete Galois orbits. In the case at hand, we have seen two Dessins in the same Galois orbit, one of which has the property that its colorings include one which contributes to the 1-point function of $(Y^2X)(YX)^2(X^2)^2(X)^3$ whereas the other Dessin does not have a coloring which contributes to the 1-point function of $(Y^2X)(YX)^2(X^2)^2(X)^3$. So we conclude that in general multi-matrix operator correlators do not receive contributions from complete Galois orbits of Dessins.

5.2 Some new combinatoric Galois invariants

We fix a number k of Matrix types. We specify a vector of positive integers $\vec{n} = (n_1, n_2, \dots, n_k)$ of length k , which determines how many matrices of each type we have. For each Dessin, we get a list of multi-matrix operators. If we take the intersection of the lists associated

with each Dessin in an orbit we get a Galois invariant. In examples where we know a set of Dessins to form a complete Galois orbit, we can compute the lists for each Dessin and then determine the intersection. To make this a powerful idea in the determination of Galois orbits we would need to find some method, which, just by considering the list of MMOs for a single Dessin can determine, without prior knowledge of the orbit structures, which of the MMOs belong to the intersection.

Similarly we can consider the union of lists over a Galois orbit, which gives another Galois invariant. The intersection appears a more economical invariant to consider.

An analogy is that the moduli field of a Dessin K_D is not Galois invariant. Although it does contain some Galois-invariant information such as the length of the Galois orbit which is equal to $\deg(K_D : \mathbb{Q})$. But the moduli field of the orbit, which is the normal extension of K_D and contains all the moduli fields of the individual Dessins, is a Galois invariant [43].

A natural question is whether these combinatoric multi-matrix Galois invariants are a complete set? The union invariant is complete. By choosing k to be as large as the number of edges in the Dessin, we can determine permutations σ_0, σ_1 which describe the Dessin. Since the S_d equivalence class of σ_0, σ_1 completely identify the Dessin, the maximal number of colors certainly determines the Galois orbit which the Dessins sits in. By using fewer colors, we may hope to extract information that identifies the orbit only and not extra information about the Dessin. It is not at all obvious that the intersection invariant is complete.

It is worth remarking that we have considered the construction of Galois invariants from lists of MMOs, but we could equally well have considered lists of CEDs, then taken intersections and unions.

We leave it to future research to determine effective ways of computing the intersection invariant, or similar invariants from lists of colored edge Dessins or multi-matrix operators, and to determine their usefulness. What is clear is that lists of CEDs and MMOs capture more detailed information about Dessins than coarse Galois invariants such as $[\sigma_0], [\sigma_1], [\sigma_0\sigma_1]$. In the following section, we will make use of this observation to translate known Galois invariants into the language of CEDs and MMOs.

5.3 Known invariants and edge-colorings of Ribbon graphs

5.3.1 Flower-shaped trees

There is a famous case of two trees, which are in different Galois orbits, but require a rather non-obvious Galois invariant to separate them [42]. Both trees have a central black vertex, and 5 white vertices joined to it. These 5 white vertices have, respectively, 1, 2, 3, 4, 5 black vertices attached to them. The ordering of these 5 white vertices is different in the two trees. According to Zapponi [53] the action of the Galois group is to permute the five petals to give a permutation in S_5 defined up to multiplication by the 5-cycle (12345), which means

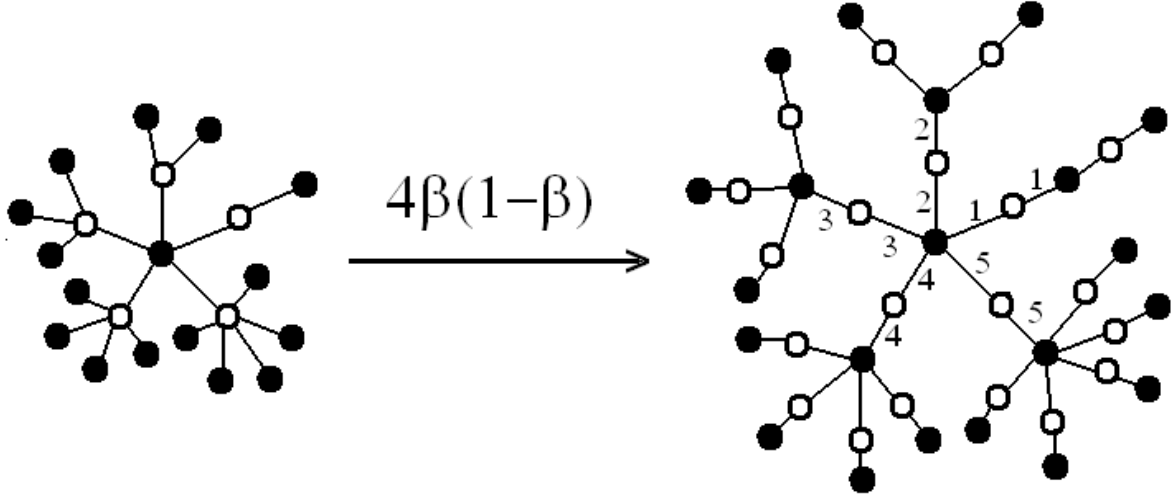


Figure 17: A multi-matrix operator from Leila Flower

that the sign of the permutation is invariant, so there are two distinct Galois orbits among Dessins of this type.

This description of the Galois invariant in terms of the sign of a permutation of the petals can be mapped to a description in terms of multi-matrix operators or colored Dessins associated to the specified Dessin.

We will use 5 types of matrices Y_1, Y_2, Y_3, Y_4, Y_5 along with the matrix X . We will focus on operators where the central vertex has these 5 Y_i . The remaining edges are labeled by X . In the list associated with the first tree, we will have

$$(Y_1 Y_2 Y_3 Y_4 Y_5)(Y_1 X)(Y_2 X^2)(Y_3 X^3)(Y_4 X^4)(Y_5 X^5)(X)(X^2)(X^3)(X^4)(X^5) \quad (5.3)$$

In the list for the second tree, the multi-matrix operator will be

$$(Y_1 Y_2 Y_3 Y_4 Y_5)(Y_2 X)(Y_1 X^2)(Y_3 X^3)(Y_4 X^4)(Y_5 X^5)(X)(X^2)(X^3)(X^4)(X^5) \quad (5.4)$$

So clearly we can express the permutation relating the two configurations in terms of a permutation relating operators in the respective lists, constrained to have Y 's at the central vertex. Hence the Galois invariant can be expressed in terms of combinatoric information about the Dessin encoded by the lists of MMOs associated to it. In the Figure 17, we show one of these trees and we also show how the tree changes when we apply $\beta \rightarrow 4\beta(\beta - 1)$, and the corresponding multi-matrix operator.

Galois orbits are understood for more general classes of trees related to the one above. If the valencies $(2, 3, 4, 5, 6)$ of outer white vertices are replaced by $(a_1, a_2, a_3, a_4, a_5)$, then we have two orbits if $a_1 a_2 a_3 a_4 a_5 (a_1 + a_2 + a_3 + a_4 + a_5)$ is a square and one orbit otherwise.

We observe that the data $(a_1, a_2, a_3, a_4, a_5)$ which is important in determining Galois orbits can also be described in terms of CEDs. Again we color the central edges Y_1, Y_2, \dots, Y_5 .

The X 's are replaced by $X_1, X_2 \dots$ with the condition that the X 's going with Y_1 have lower indices than those going with Y_2 etc. Then we have $(Y_1 X_1), (Y_2 X_2 X_3) \dots$. Now if we keep the colors of edges connected to the central vertex fixed and let colorings vary only in the cycle containing Y_i along with X 's we get the numbers $p_i!$. From this we can extract the $a_i = p_i + 1$. The condition on $a_1 a_2 \dots a_5 (a_1 + \dots + a_5)$ can now be expressed in terms of these multiplicities of CEDs or of MMOs.

5.3.2 Galois orbits for $K_{n,n}$

Consider Dessins with underlying graph consisting of n black vertices and n white vertices. To get the underlying graph from a Dessin, just forget the cyclic ordering at each vertex. Further restrict to the case where each of the n black vertices is connected to each white vertex by exactly one edge. This is called a complete bi-partite graph $K_{n,n}$. Further restrict to the case $n = p^e$ for a prime p which is not equal to 2 and positive integer e . The set of all Dessins with this underlying graph are *regular* and the structure of their Galois orbits is known [66]. Regular Dessins have an automorphism group which is transitive, i.e when viewed as a subgroup of S_d can map any integer from $\{1, \dots, d\}$ to any other. There are p^{e-1} distinct Dessins. These are organized into orbits parameterized by integers f from the set $\{1, 2, \dots, e\}$. For each f consider integers u from the set $\{1, 2, \dots, p^{e-f}\}$, which are not divisible by p . There are $\varphi(p^{e-f})$ such choices, where φ is the Euler totient function. Each choice leads to a curve $X_{p,e,f,u}$ and a Belyi map to \mathbb{P}^1 . Using an identity $\sum_f \varphi(p^{e-f}) = p^{e-1}$ we have the number of Dessins stated above.

The construction of these Dessins is given a group theoretic description in [66]. It is useful, for our purposes, to find explicitly the description in terms of permutations σ_0, σ_1 . We know from the description above that the degree of the map is n^2 . Above each of 0 and 1, there are n ramification points each with degree n . So we are looking for permutations in S_{n^2} .

Define $q = p^f + 1$, and consider

$$\begin{aligned} h(nk + 1 + i) &= nk + 1 + (i + 1)_n \\ g^{-1}(nk + 1 + i) &= n(k + 1)_n + 1 + (qi)_n \\ g(nk + i + 1) &= n(k - 1)_n + 1 + \left(\frac{i}{q}\right)_n \end{aligned} \tag{5.5}$$

with $i = 0 \dots n - 1$, $k = 0, \dots, (n - 1)$. We can check that these satisfy

$$\begin{aligned} gh &= h^q g \\ g^n &= h^n = 1 \end{aligned} \tag{5.6}$$

These equations (5.6) are the fundamental equations used to describe the Dessins in [66, 67]. We can also check $(gh)^n = 1$.

The check for h^n is trivial. For g^n one writes out

$$g^{-n}(nk + 1 + i) = n(k + n)_n + 1 + (q^n i)_n \quad (5.7)$$

$(q^n i)_n = ((q^n)_n (i)_n)_n = i$. Using Lemma 6 of [67] we have $(q^n)_n = 1$. We can also write out the action of (gh) .

$$gh(nk + 1 + i) = n(k - 1)_n + 1 + \left(\frac{i + 1}{q}\right)_n \quad (5.8)$$

It is clear from this formula that $n(k + 1)_n \leq gh(x) \leq n(k + 2)_n$ for $nk \leq x \leq n(k + 1)$. We can also check that gh obeys $(gh)^n = 1$. This proves that gh consists of n cycles of length n .

From these fundamental permutations we get the Dessins [66] as

$$\begin{aligned} \sigma_0 &= g^u \\ \sigma_1 &= (gh)^u \end{aligned} \quad (5.9)$$

As explained in the previous section 5.1, if we use the maximal number of colors, we can certainly reconstruct σ_0, σ_1 . The degree of the map is n^2 , the cycle decompositions of σ_0, σ_1 are $[n^n]$, so we can extract $n = p^e$. To extract f, u from the permutations, we calculate from the basic relations (5.6) that

$$\sigma_1 \sigma_0^{-1} = (\sigma_0^{-1} \sigma_1)^{q^u} \quad (5.10)$$

Hence the colored Dessins with maximal colors allow us to recover σ_0, σ_1 , and by comparing $\sigma_1 \sigma_0^{-1}$ and $\sigma_0^{-1} \sigma_1$ we extract q, u , and in turn we extract f from the definition $q = p^f + 1$.

This gives a proof-of-principle that the Galois invariants p, e, f can be extracted using colorings of the Dessins. We have used the maximal number of colors which allow us to directly construct σ_0, σ_1 . It would be interesting to find the minimal number of edge-colors which can reconstruct the data p, e, f .

6 Summary and Outlook

Our motivation was to apply the logic of the string theory of 2dYM where Hurwitz space was found to play a central role, to the case of correlators in hermitian matrix models.

Summary of Key points

1. By using diagrammatic tensor space calculations, we showed that correlators of arbitrary multi-traces of the 1-matrix model at generic couplings can be mapped to counting problems involving certain triples of permutations. This lead to an interpretation in terms of Hurwitz numbers. The matrix model has a dual string theory interpretation in terms of a target space \mathbb{P}^1 , which localizes on holomorphic maps with three branch points. Note that, in contrast to the traditional non-critical string interpretation, this requires no double-scaling limit for a continuum interpretation.

2. We used results in the Matrix model literature to get explicit results on Hurwitz numbers with three branch points. We believe these results on Hurwitz numbers are new and these calculations should admit many generalizations.
3. Exploiting one of Grothendieck's remarks [68], we highlighted the fact that the absolute Galois group organizes the Feynman graphs of the 1-matrix model.
4. We observed that edge-colorings of Grothendieck Dessins arise when we consider correlators of the multi-matrix models. The counting of these edge-colored Dessins is related to counting of triples of permutations in S_d with equivalences defined by subgroups.
5. We argued that multi-matrix models at generic couplings are related to a continuum string theory defined by sheaves over the Hurwitz space of branched covers with 3 branch points.
6. We used edge-colorings and related lists of multi-matrix operators to define new invariants of the Galois action on Dessins.
7. We related known Galois invariants to edge-colorings and lists.

We will discuss extensions of this work, connections to recent literature and intriguing puzzles under three main headings.

- 1. Hurwitz spaces, $\mathcal{M}_{g,n}$ and topological strings,
- 2. The target space of the string dual of Matrix models.
- 3. The absolute Galois group $Gal(\bar{\mathbb{Q}}/\mathbb{Q})$.

Hurwitz spaces and topological strings

The computation (section 2.5), using existing Matrix model literature, of explicit Hurwitz numbers with general ramification profiles over two branch points but with simple ramification points over one branch point, can clearly be generalized. The computation of explicit Hurwitz numbers [69] for a different case, namely where all branch points have simple ramification profile of type $[21^{d-2}]$ has been related recently to intersection theory over $\mathcal{M}_{g,n}$ [57]. An intersection theory approach to more general branching data for the case of genus zero world-sheet is available [70]. Elaborating on the connection with the results of section 2.5 would be interesting.

In the recent work [71] exact answers for generating functions of correlators in the hermitian matrix correlators were constructed. Given the results of section 2, these can be interpreted as generating functions for Hurwitz numbers.

Different spacetimes from Refinements of Hurwitz counting

In this article we have focused on Matrix models which are zero dimensional quantum field

theories. Similar calculations in higher dimensional conformal field theories, in the context of the Zamolodchikov inner product on the space of all gauge invariant operators of interest in AdS/CFT, express correlators in terms of symmetric group data [16, 17, 18, 19, 20, 21, 22, 72]. In [17] (for example section 5 and 8) there are computations showing how different refinements of symmetric group counting problems (hence Hurwitz space combinatorics) are weighted with different space-time dependences of correlators. This suggests that spacetime might emerge from refinements of Hurwitz counting problems. Another recent AdS/CFT development in connection with Hurwitz spaces is the work [73].

The target space of the dual string theory for the one-Matrix model

Our work provides a continuum string interpretation of one-Matrix model correlators at for arbitrary parameters of the potential $V(X)$. The target space is \mathbb{P}^1 . The maps we encounter involve those where there are precisely three branch points on the target space. The ramification points in the inverse image of the branch points are determined by the parameters of the potential and the observable inserted (see section 2.6). Using the Belyi theorem, these curves and maps are defined over $\bar{\mathbb{Q}}$. This suggests that the target space is really $\mathbb{P}^1(\bar{\mathbb{Q}})$.

The traditional spacetime interpretation of the minimal strings is that we have one real dimension : which can be viewed as the Liouville direction, or as the eigenvalue direction of the Matrix model. A two dimensional target space, which is a Riemann surface semi-classically but becomes a \mathbb{P}^1 non-perturbatively was discussed in [32]. The \mathbb{P}^1 target space is compatible with our interpretation. While the observables we have considered are powers of traces, the ones considered in [32] involve determinants. The geometrical structure we have developed is Hurwitz spaces, whereas the geometries related to the integrable structures there are infinite dimensional Grassmannians. The Matrix theory transformation between the two types of observables (see expressions in 2.6) therefore seems to be capturing some interesting geometrical relations between Hurwitz spaces for 3-branch point maps and Grassmannians. It would be very interesting to articulate that more precisely.

In the picture developed in this paper, the double-scaling limits can be viewed as arising by tuning the couplings of the different ramification points which are present in the exponential of the potential (2.50). So the string theory on $\mathbb{P}^1(\bar{\mathbb{Q}})$ contains these different double scaled limits when the couplings of ramification points are tuned. This has some similarity to the phase transition in 2dYM which was interpreted in terms of “condensation of branch points” [75].

Our claim that we have the string theory for the 1-matrix model at generic coupling is based on treating the partition function as a perturbation of the Gaussian model. In cases where the perturbation series has a finite radius of convergence, one could argue that beyond the radius of convergence, the description in terms of string theory on \mathbb{P}^1 is not valid. This is reminiscent of the discussion of phase transitions for 2dYM on the sphere [74]. Quite generally one can view the integral as a formal series rather than a convergent series, so the

picture of $\mathbb{P}^1(\bar{\mathbb{Q}})$ holds in this interpretation (for relations between the convergent series and formal series interpretations see [76]).

String theory over fields other than \mathbb{C} were discussed in the past, especially p-adic strings [77, 78] and they have received renewed interest recently in the context of tachyon condensation [79]. The observations in this paper are suggesting that old-matrix models at generic couplings admit such an interpretation as string theory over $\bar{\mathbb{Q}}$ with target space $\mathbb{P}^1(\bar{\mathbb{Q}})$. Is there a concrete construction of such a string ? Since a lot of algebraic geometry such as that of Hurwitz spaces and $\mathcal{M}_{g,n}$ (see for example [80]) is done over general algebraically closed fields, it is tempting to believe that the answer is yes. Is there an explicit construction of a worldsheet string path integral over $\bar{\mathbb{Q}}$ and the string field theory on $\mathbb{P}^1(\bar{\mathbb{Q}})$?

The absolute Galois group

The Galois group $Gal(\bar{\mathbb{Q}}/\mathbb{Q})$ is of fundamental interest in number theory. It has no known explicit description in terms of generators and relations for example. For mathematicians, the interest in the faithful action of $Gal(\bar{\mathbb{Q}}/\mathbb{Q})$ on Dessins comes from the fact that it is a way to learn about the mysterious group itself. The coarser invariants of the Galois action, such as the conjugacy classes of the permutations in the description in terms of triples of permutations, do not suffice to distinguish distinct Galois orbits.

We have been lead, by considering Feynman diagrams of multi-matrix models, to study the Galois action on Dessins by doing what infants would naturally do, namely color the edges. Coloring the edges captures combinatoric information about the Dessins ⁵. Some of this combinatoric information was related in section 5 to known mathematical Galois invariants which contain information about how Dessins fit into Galois orbits. We also defined new invariants in terms of intersections and unions over Galois orbits of colored-edge Dessins. The union-invariants, with sufficiently many colors, are complete, in the sense that they can certainly contain enough information to characterize orbits. However, they contain in a sense too much information and computing them would seem to require scanning entire orbits. The intersection-invariant by contrast is local in that it is a property of the set of colorings of any single Dessin. An interesting problem is to find out if the intersection invariant is useful for distinguishing orbits that cannot be distinguished by other methods. More generally, we can ask whether there exists any complete set of local invariants, which can be defined in terms of the colorings of a given Dessin, and are complete in that they can always tell whether a pair of Dessins are in the same orbit or not.

⁵Incidentally, another variation on this theme is that working with complex matrix models amounts to coloring the edges as well as giving them an arrow.

Acknowledgements

We thank Amir Kashani Poor, Yusuke Kimura, Vishnu Jejjalla, David Madore, Rodolfo Russo, David Turton for useful discussions/correspondence. SR is supported by an STFC grant ST/G000565/1. RdMK is supported by the South African Research Chairs Initiative of the Department of Science and Technology and National Research Foundation.

A Glossary and key facts

Absolute Galois group

The Galois group of the closure $\bar{\mathbb{Q}}$ of the rationals \mathbb{Q} . It is the subgroup of the automorphism group of $\bar{\mathbb{Q}}$ which leaves \mathbb{Q} fixed.

Automorphisms

$Aut(\sigma_0, \sigma_1)$ is the automorphism group of a set of triples $\sigma_0, \sigma_1, (\sigma_0\sigma_1)^{-1}$ (defined in section (2.1)), $AutD$ the automorphism group of a Dessin D , $Autf$ the automorphism group of a holomorphic map f (defined in section 2.3). Under the correspondence between triples, Dessins and holomorphic maps with 3 branch points, these are isomorphic.

Belyi map

A map from $\beta : \Sigma_h \rightarrow \mathbb{P}^1$ with three branch points at $0, 1, \infty$ from a curve Σ_h (which is interpreted as the string worldsheet). The image \mathbb{P}^1 is the target space of the string theory.

Belyi's theorem

All Belyi maps are defined over $\bar{\mathbb{Q}}$. The underlying curve can be defined by algebraic equations involving algebraic number coefficients and the map itself involves only such coefficients.

Bipartite graph

A graph with two types of vertices : Black and white. Black vertices are connected to white. The white vertices correspond to ramification points above 1. These graphs correspond to triples of permutations. The first permutation σ_0 described by the permutation of labeled edges around the black vertices as specified by the cyclic order which comes with each vertex. The second permutation σ_1 describes permutations around the white vertices. See [42, 43, 44].

Branch point

A point on the target space, such that inverse image contains one or more points where the derivative vanishes. In terms of local coordinates w on the target there is at least one point in the inverse image of $w = 0$, with local coordinate z on the worldsheet where the map is described by $w = z^i$ with $i > 1$. *CARE* : A branch point is a point on the target (unlike a ramification point).

Clean Belyi map

Belyi maps such that all ramification indices over the point 1 are simple (look like $w = z^2$ in local coordinates). These maps are the sorts that arise in the string description when we consider correlators in perturbed Gaussian matrix models.

Clean Dessins

The white vertices each have two incident edges. Clean Dessins correspond to clean Belyi maps.

Clean Dessins \leftrightarrow Gaussian Matrix model

The clean Dessins come from the Wick contractions in a Gaussian matrix model. Each trace $\text{tr}X^k$ gives a black vertex with k edges. Each propagator is associated with a white vertex. See section 3.3.

Colored-Edge-Dessins (CEDs)

They are the Feynman graphs obtained in the multi-Matrix models, e.g a matrix model (Gaussian or perturbed Gaussian) with different types of matrices $X, Y, Z \dots$. They are related to triples of permutations in S_d with equivalences defined by subgroups of S_d (see definition in section 4).

Complete bi-partite graph

Every white vertex is connected to every black vertex. Special case of interest to us in section 5.3.2 is $K_{n,n}$ where there is an equal number of black and white vertices. Many different Dessins can have the same underlying graph. Physicists are familiar with this fact from Feynman diagrams in matrix models, where different connections between the same vertices in a Feynman graph can change the N dependence of the diagram.

Correlators of Matrix operators

Correlators of the matrix operators are defined by insertion of the matrix operator in a hermitian matrix integral with a Gaussian action or perturbed Gaussian with a general potential parametrised by couplings g_3, g_4, \dots . After interating the Matrix we have the correlator.

Delta function over symmetric group

For $\sigma \in S_d$ we define $\delta_{S_d}(\sigma) = 1$ if σ is the identity permutation, and $\delta_{S_d}(\sigma) = 0$ otherwise. By linearity this extends to a delta-function on the group algebra. This arises in counting branched covers (section (2.1)).

Double Line diagrams, Ribbon graphs, Grothendieck Dessins

Physicists usually use double line diagrams to describe the Feynman graphs of one-Matrix models. If we collapse the double lines to single lines, there is no loss of information as long as we keep track of a cyclic order at the vertices, inherited from an oriented surface supporting the graph. These are ribbon diagrams or Grothendieck Dessins. In this paper, we mapped the computation of correlators in the Matrix model directly to counting of certain triples of permutations, which are well-known to be the combinatoric description of Dessins.

From Belyi map to Dessin

The Dessin corresponding to a Belyi map is obtained as the inverse image of $[0, 1]$ under the Belyi map. Points over 1 are marked with white vertices and points over 0 are marked with black vertices.

Galois action on Dessins, or triples of permutations

Dessins or triples of permutations correspond to worldsheets and maps to the sphere \mathbb{P}^1 defined over $\bar{\mathbb{Q}}$. The Galois group acts on the elements of $\bar{\mathbb{Q}}$ and hence on Dessins or triples.

Galois invariants of action on Dessins or triples

Examples of invariants are the conjugacy classes $[\sigma_0], [\sigma_1], [\sigma_\infty]$, the automorphism group $Aut(D)$. Finer invariants are discussed in section (5).

Galois closure of rationals $\bar{\mathbb{Q}}$

The Galois closure of the rationals contains the solutions of all possible polynomial equations in a variable x with coefficients which are rational, i.e in \mathbb{Q} .

Holomorphic map to \mathbb{P}^1

A map $f : \Sigma_h \rightarrow \mathbb{P}^1$ from a Riemann surface of genus h to the sphere \mathbb{P}^1 . Fixing a small disc on the target space described by a local coordinate w , the inverse image consists of a number of discs. Restricting to one disc, the map looks like $w = z^i$. Summing over the indices i , we get the degree d of the map.

Matrix operators

When computing a matrix integral over a matrix X , with a Gaussian or more general weight, observables of interest include arbitrary moments built using traces and multi-traces such as $(tr(X))^3, trX^3$. We call these observables matrix operators. Multi-trace operators with m copies of X are related to conjugacy classes of S_m (see section 2.2).

Multi-Matrix operators (MMOs)

They are traces of matrices involving multiple matrix types, e.g $trX^2trY^2, trX^2Y^2, trXYXY$. Correlators of these multi-matrix multi-traces are the observables of interest in multi-matrix models.

Notation for conjugacy class of a permutation

If σ is a permutation, $[\sigma]$ is the conjugacy class of the permutation, which is also the cycle structure of the permutation. Conjugacy classes of S_d are specified by partitions of d .

Number field

Fields consists of a set of elements together with four operations, addition, subtraction, multiplication and division by nonzero elements. The rational numbers \mathbb{Q} , together with their usual operations, form a number field.

$\mathbb{P}^1(\bar{\mathbb{Q}})$

The projective line over the field $\bar{\mathbb{Q}}$ is defined as the set of one-dimensional subspaces of the two-dimensional vector space $\bar{\mathbb{Q}}^2$.

Ramification point

A point on the world-sheet where the derivative of the map vanishes. In the local description

in terms of $w = z^i$, we have $i \geq 1$. *CARE*: A ramification point is a point on the worldsheet (unlike a branch point). This usage of branch point and ramification point is conventional in mathematical literature on branched covers, but not by no means universal.

Ramification profiles

A set of positive integers describing the ramifications of all points in the inverse image of a branch point. The ramification profile of a branch point for a map of degree d is a partition of d , which corresponds to conjugacy classes of S_d .

Riemann's existence theorem

Relates (equivalence classes of) a sequence of permutations $\sigma_1, \sigma_2, \dots, \sigma_L$ obeying $\sigma_1 \sigma_2 \dots \sigma_L = 1$ to (equivalence classes of) holomorphic maps to \mathbb{P}^1 target with L branch points (see section 2.1).

Simple Hurwitz space

This is the space of holomorphic maps from worldsheet to target space, where the ramification profiles over all branch points are of the form $[21^{d-2}]$. This is the focus in a number of discussion of Hurwitz spaces in the context of topological string theory and algebraic geometry. It is not the main subject of this paper.

Triples of permutations

A set of three permutations $\sigma_0, \sigma_1, \sigma_\infty \in S_d$, such that $\sigma_0 \sigma_1 \sigma_\infty = 1$. Equivalence of triples is defined in section 2.1. The computation of any observable in Gaussian or perturbed Gaussian matrix model can be mapped to a summation over equivalence classes of these triples (see section 2.3).

Wick's theorem

A combinatoric rule which allows the computation of correlators in a Gaussian matrix model and its perturbations by a general potential (see 2.15). It involves a sum over products of *Wick contractions*.

References

- [1] E. Brezin and V. A. Kazakov, "Exactly solvable field theories of closed strings," Phys. Lett. B **236** (1990) 144.
- [2] D. J. Gross and A. A. Migdal, "A nonperturbative treatment of two-dimensional quantum gravity," Nucl. Phys. B **340** (1990) 333.
- [3] M. R. Douglas and S. H. Shenker, "Strings In Less Than One-Dimension," Nucl. Phys. B **335** (1990) 635.
- [4] E. Witten, "On the Structure of the Topological Phase of Two-Dimensional Gravity," Nucl. Phys. B **340**, 281 (1990).

- [5] R. Dijkgraaf and E. Witten, “Mean Field Theory, Topological Field Theory, and Multi-matrix Models,” Nucl. Phys. B **342**, 486 (1990).
- [6] P. H. Ginsparg and G. W. Moore, arXiv:hep-th/9304011.
- [7] J. Polchinski, “What is string theory?,” arXiv:hep-th/9411028.
- [8] P. Di Francesco, P. H. Ginsparg and J. Zinn-Justin, “2-D Gravity and random matrices,” Phys. Rept. **254** (1995) 1 [arXiv:hep-th/9306153].
- [9] D. J. Gross, “Two-dimensional QCD as a string theory,” Nucl. Phys. B **400** (1993) 161 [arXiv:hep-th/9212149].
D. J. Gross and W. Taylor, Nucl. Phys. B **400**, 181 (1993) [arXiv:hep-th/9301068],
D. J. Gross and W. Taylor, Nucl. Phys. B **403**, 395 (1993) [arXiv:hep-th/9303046].
- [10] Y. Kimura and S. Ramgoolam, “Holomorphic maps and the complete $1/N$ expansion of 2D $SU(N)$ Yang-Mills,” JHEP **0806** (2008) 015 [arXiv:0802.3662 [hep-th]].
- [11] A. Pakman, L. Rastelli and S. S. Razamat, “Extremal Correlators and Hurwitz Numbers in Symmetric Product Orbifolds,” Phys. Rev. D **80** (2009) 086009 [arXiv:0905.3451 [hep-th]].
- [12] M. Marino, R. Schiappa and M. Weiss, “Nonperturbative Effects and the Large-Order Behavior of Matrix Models and Topological Strings,” arXiv:0711.1954 [hep-th].
- [13] S. Cordes, G. W. Moore and S. Ramgoolam, Commun. Math. Phys. **185** (1997) 543 [arXiv:hep-th/9402107].
- [14] S. Cordes, G. W. Moore and S. Ramgoolam, “Lectures On 2-D Yang-Mills Theory, Equivariant Cohomology And Topological Field Theories,” Nucl. Phys. Proc. Suppl. **41**, 184 (1995) [arXiv:hep-th/9411210].
- [15] S. Ramgoolam, “Wilson loops in 2-D Yang-Mills: Euler characters and loop equations,” Int. J. Mod. Phys. A **11**, 3885 (1996) [arXiv:hep-th/9412110].
- [16] S. Corley, A. Jevicki and S. Ramgoolam, “Exact correlators of giant gravitons from dual $N = 4$ SYM theory,” Adv. Theor. Math. Phys. **5**, 809 (2002) [arXiv:hep-th/0111222].
- [17] S. Corley and S. Ramgoolam, “Finite factorization equations and sum rules for BPS correlators in $N = 4$ SYM theory,” Nucl. Phys. B **641**, 131 (2002) [arXiv:hep-th/0205221].
- [18] R. de Mello Koch, J. Smolic and M. Smolic, “Giant Gravitons - with Strings Attached (I),” JHEP **0706**, 074 (2007) [arXiv:hep-th/0701066],

- R. de Mello Koch, J. Smolic and M. Smolic, JHEP **0709**, 049 (2007) [arXiv:hep-th/0701067].
- D. Bekker, R. de Mello Koch and M. Stephanou, JHEP **0802** (2008) 029 [arXiv:0710.5372 [hep-th]].
- [19] T. W. Brown, P. J. Heslop and S. Ramgoolam, “Diagonal multi-matrix correlators and BPS operators in N=4 SYM,” JHEP **0802**, 030 (2008) [arXiv:0711.0176 [hep-th]],
T. W. Brown, P. J. Heslop and S. Ramgoolam, JHEP **0904**, 089 (2009) [arXiv:0806.1911 [hep-th]].
- [20] Y. Kimura and S. Ramgoolam, “Branes, Anti-Branes and Brauer Algebras in Gauge-Gravity duality,” JHEP **0711**, 078 (2007) [arXiv:0709.2158 [hep-th]].
Y. Kimura and S. Ramgoolam, Phys. Rev. D **78** (2008) 126003 [arXiv:0807.3696 [hep-th]].
- [21] R. de Mello Koch, “Geometries from Young Diagrams,” JHEP **0811**, 061 (2008) [arXiv:0806.0685 [hep-th]].
- [22] R. Bhattacharyya, S. Collins and R. d. M. Koch, “Exact Multi-Matrix Correlators,” JHEP **0803**, 044 (2008) [arXiv:0801.2061 [hep-th]].
- [23] G. Belyi, “On Galois extensions of a maximal cyclotomic field,” Math. USSR Izv. **14** (1979), 247-256.
- [24] See for example the book review “Inverse Galois Theory,” H. Volklein, Bulletin of the AMS, **38** (2000), 235-243.
- [25] T. W. Brown, “Permutations and the Loop,” JHEP **0806** (2008) 008 [arXiv:0801.2094 [hep-th]].
- [26] R. de Mello Koch, N. Ives and M. Stephanou, “Correlators in Nontrivial Backgrounds,” Phys. Rev. D **79** (2009) 026004 [arXiv:0810.4041 [hep-th]].
- [27] Y. Kimura, S. Ramgoolam and D. Turton, “Free particles from Brauer algebras in complex matrix models,” arXiv:0911.4408 [hep-th].
- [28] E. Brezin, C. Itzykson, G. Parisi and J. B. Zuber, “Planar Diagrams,” Commun. Math. Phys. **59**, 35 (1978).
- [29] I. Goulden, D. Jackson and R. Vakil, “Towards the geometry of double Hurwitz numbers,” <http://arxiv.org/pdf/math/0309440>
- [30] G. M. Cicuta, L. Molinari and E. Montaldi, “Multicritical points in Matrix Models,” J. Phys. A **23**, L421 (1990).
- [31] Symmetrica can be used online at:
<http://www.algorithm.uni-bayreuth.de/en/research/SYMMETRICA/>

- [32] J. M. Maldacena, G. W. Moore, N. Seiberg and D. Shih, “Exact vs. semiclassical target space of the minimal string,” *JHEP* **0410** (2004) 020 [arXiv:hep-th/0408039].
- [33] T. Banks, M. R. Douglas, N. Seiberg and S. H. Shenker, “Microscopic and Macroscopic Loops in Nonperturbative Two-Dimensional Gravity,” *Phys. Lett. B* **238**, 279 (1990),
G. W. Moore and N. Seiberg, *Int. J. Mod. Phys. A* **7**, 2601 (1992),
I. K. Kostov, *Phys. Lett. B* **266**, 42 (1991).
- [34] D. Gaiotto, “Long strings condensation and FZZT branes,” arXiv:hep-th/0503215.
A. Mukherjee and S. Mukhi, *JHEP* **0607** (2006) 017 [arXiv:hep-th/0602119].
- [35] M. Marino, “Les Houches lectures on matrix models and topological strings,” arXiv:hep-th/0410165.
- [36] R. Dijkgraaf and C. Vafa, *Nucl. Phys. B* **644**, 3 (2002) [arXiv:hep-th/0206255].
- [37] J. Ambjorn, J. Jurkiewicz and Yu. M. Makeenko, “Multiloop correlators for two-dimensional quantum gravity,” *Phys. Lett. B* **251**, 517 (1990).
- [38] O. Ganor, J. Sonnenschein and S. Yankielowicz, *Nucl. Phys. B* **434** (1995) 139 [arXiv:hep-th/9407114].
Y. Sugawara, *Mod. Phys. Lett. A* **11** (1996) 1675 [arXiv:hep-th/9601099].
F. Dubath, S. Lelli and A. Rissone, *Int. J. Mod. Phys. A* **19** (2004) 205 [arXiv:hep-th/0211133].
- [39] G. 't Hooft, “A Planar Diagram Theory for Strong Interactions,” *Nucl. Phys. B* **72** (1974) 461.
- [40] E. Looijenga, Intersection theory on Deligne-Mumford compactifications, *Seminaire Bourbaki*, 1992-1993, exp. no. 768, pp. 187-212
- [41] M. Bauer and C. Itzykson, “Triangulations” in [47]
- [42] Leila Schneps, “Dessins d’enfants on the Riemann sphere” *London Math. Soc. Lect. Notes* 200, CUP 1994
- [43] S. K. Lando and A. K. Zvonkin, “Graphs on Surfaces and their applications,” *Encyclopaedia of Mathematical Sciences, Low dimensional Topology II*, Volume 141, Springer 2003
- [44] P. Joubert, “Geometric actions of the absolute Galois group,” *Masters Thesis*, University of Stellenbosch, 2006.
- [45] G. Jones and M. Streit “Galois groups, monodromy groups and cartographic groups,” in [46]

- [46] L. Schneps and P. Lochak, “Geometric Galois actions 2. The inverse Galois problem, moduli spaces and Mapping class groups,” Lon. Math. Soc. Lecture Note Series 243.
- [47] L. Schneps, The Grothendieck theory of Dessins d’Enfants, London Mathematical Society Lecture Notes Series 200.
- [48] See for example
http://en.wikipedia.org/wiki/Dessin_d'enfant
- [49] E. Witten, “Perturbative gauge theory as a string theory in twistor space,” Commun. Math. Phys. **252** (2004) 189 [arXiv:hep-th/0312171].
- [50] Toru Komatsu “Belyi Function whose Grothendieck Dessin is a Flower Tree with Two Ramification Indices,” Math. J. Okayama Univ. **47** (2005), 119131.
- [51] This is easily computed using PARI, an open source computer algebra system freely available from <http://pari.math.ubordeaux.fr/>.
- [52] J.S. Milne, “Fields and Galois Theory” course notes, example 4.6 page 38.
- [53] L. Zapponi, Lecture at MSRI available at
<http://www.msri.org/publications/ln/msri/1999/gactions/zapponi/1/banner/03.html>
- [54] L. Zapponi, “Fleurs, arbres, et cellules : un invariant galoisien pour une famille d’arbres,” Compositio Mathematica **122**, 113 -133, 2000.
- [55] M. Mulase, M. Penkava, “Ribbons graphs, quad differentials, curves over $\bar{\mathbb{Q}}$,” math-ph/9811024.
- [56] M. Kontsevich, “Intersection theory on the moduli space of curves and the Matrix Airy function,” Comm. Math. Phys. **147**, Number 1, June 1992.
- [57] T. Ekedahl, S. Lando, M. Shapiro, A. Vainshtein, “Hurwitz numbers and intersections on moduli spaces of curves” <http://arxiv.org/abs/math/0004096>
- [58] S. K. Ashok, F. Cachazo and E. Dell’Aquila, arXiv:hep-th/0611082.
- [59] R. Gopakumar, Phys. Rev. D **70** (2004) 025009 [arXiv:hep-th/0308184].
- [60] T. Eguchi and S. K. Yang, “The Topological CP^1 model and the large N matrix integral,” Mod. Phys. Lett. A **9**, 2893 (1994) [arXiv:hep-th/9407134],
T. Eguchi, K. Hori and S. K. Yang, Int. J. Mod. Phys. A **10**, 4203 (1995) [arXiv:hep-th/9503017].
- [61] T. Koppe, “Notes on sheaf theory and the Fourier-Mukai transform”
<http://www.maths.ed.ac.uk/~s0571100/FMNotes.pdf>

- [62] E. Witten, “The N Matrix Model And Gauged WZW Models,” Nucl. Phys. B **371** (1992) 191.
- [63] M. Aganagic, H. Ooguri, N. Saulina and C. Vafa, Nucl. Phys. B **715** (2005) 304 [arXiv:hep-th/0411280].
 N. Caporaso, M. Cirafici, L. Griguolo, S. Pasquetti, D. Seminara and R. J. Szabo, JHEP **0601** (2006) 035 [arXiv:hep-th/0509041].
 M. Aganagic, D. Jafferis and N. Saulina, JHEP **0612** (2006) 018 [arXiv:hep-th/0512245].
- [64] V. A. Kazakov, “Ising model on a dynamical planar random lattice: Exact solution,” Phys. Lett. A **119**, 140 (1986).
- [65] Wikipedia article on “Dessin D’Enfant” available at http://en.wikipedia.org/wiki/Dessin_d'enfant
- [66] G.A. Jones, M. Streit and J. Wolfart, “ Galois action on families of generalised Fermat curves, ” Journal of Algebra **307**, (2007) 829-840.
- [67] G.A. Jones, R. Nedela, M. Skoveria, “ Regular embeddings of $K_{n,n}$ where n is an odd prime power,” European Journal of Combinatorics, **28**, (2007) 1863-1875.
- [68] A. Grothendieck, “Esquisse d’un Programme,” in [47]
- [69] M. J. Crescimanno and W. Taylor, “Large N phases of chiral QCD in two-dimensions,” Nucl. Phys. B **437** (1995) 3 [arXiv:hep-th/9408115].
- [70] S. Shadrin, “Geometry of meromorphic functions and intersections on moduli spaces of curves,” <http://arxiv.org/pdf/math/0209282>
- [71] A. Morozov and S. Shakirov, “Exact 2-point function in Hermitian matrix model,” JHEP **0912**, 003 (2009) [arXiv:0906.0036 [hep-th]].
- [72] T. W. Brown, R. de Mello Koch, S. Ramgoolam and N. Toumbas, “Correlators, probabilities and topologies in $N = 4$ SYM,” JHEP **0703**, 072 (2007) [arXiv:hep-th/0611290].
- [73] A. Pakman, L. Rastelli and S. S. Razamat, “A Spin Chain for the Symmetric Product CFT_2 ,” arXiv:0912.0959 [hep-th].
- [74] M. R. Douglas and V. A. Kazakov, “Large N phase transition in continuum QCD in two-dimensions,” Phys. Lett. B **319**, 219 (1993) [arXiv:hep-th/9305047].
- [75] W. Taylor, “Counting strings and phase transitions in 2-D QCD,” arXiv:hep-th/9404175.
- [76] B. Eynard, “Large N expansion of convergent matrix integrals, holo morphic anomalies, and background independence,” JHEP **0903** (2009) 003 [arXiv:0802.1788 [math-ph]].

- [77] P. G. O. Freund and M. Olson, “Nonarchimedean Strings,” *Phys. Lett. B* **199** (1987) 186.
- [78] I. V. Volovich, “p-Adic String,” *Class. Quant. Grav.* **4** (1987) L83.
- [79] D. Ghoshal and A. Sen, “Tachyon condensation and brane descent relations in p-adic string theory,” *Nucl. Phys. B* **584** (2000) 300 [arXiv:hep-th/0003278].
- [80] P. Deligne and D. Mumford, “The irreducibility of the space of curves of a given genus,” *Publications Mathematiques de L’IHS*, Volume 36, Number 1, January 1969.